Reviewed Preprint
v1 • July 13, 2026
Not revised

For correspondence:
skuroda@bs.s.u-tokyo.ac.jp

Competing interests: No competing interests declared

Funding: See page 27

Reviewing editor: Alyssa M Wilson, Icahn School of Medicine at Mount Sinai, United States

Metabolic Trans-Omic Analysis Reveals Key Regulatory Disruption of Energy Metabolism in Alzheimer's Disease

Tomoharu Katayama[1], Hikaru Sugimoto[2], Keigo Morita[2,3], Hirohisa Watanabe[4], Shinya Kuroda[2,3]

[1]Department of Medicine, Faculty of Medicine, The University of Tokyo, Tokyo, Japan • [2]Department of Biological Sciences, Graduate School of Science, The University of Tokyo, Tokyo, Japan • [3]Molecular Genetics Research Laboratory, Graduate School of Science, The University of Tokyo, Tokyo, Japan • [4]Department of Neurology, Fujita Health University School of Medicine, Toyoake, Japan

eLife Assessment

This study presents a **useful** application of trans-omic network analyses to existing human brain datasets, generating systems-level insights into metabolic dysregulation in Alzheimer's disease. Overall, the authors' analytical choices are **solid**, with appropriate use of existing data and methods, and with many of their results confirming previous findings. However, some of the authors' key claims, related to previously unknown details of regulatory relationships, are only partially supported due to limitations in dataset cell-type resolution and network robustness, as well as a lack of functional validation. This work will be of interest to cellular or systems neurobiologists studying Alzheimer's disease and could serve as a helpful starting point for future work.

[Editors' note: this paper was reviewed by *Review Commons*.]

https://doi.org/10.7554/eLife.111228.1.sa2

Abstract

Alzheimer's disease (AD), a leading cause of dementia, has been recognized as a disease with profound metabolic dysregulation. However, a systems-level view of metabolic regulation across multiple omic modalities in AD remains elusive. Here, we integrated public multi-omic datasets (transcriptome, proteome, and metabolome) from the dorsolateral prefrontal cortex of AD patients and controls. By leveraging existing molecular biological knowledge, we reconstructed a multi-layered metabolic regulatory network to systematically map the potential interplay among mRNAs, proteins, and metabolites in AD. Our analysis revealed a putative coordinated downregulation of energy producing pathways, including the TCA cycle, oxidative phosphorylation, and ketone body metabolism, driven by reduced enzyme abundance and inhibitory allosteric effects. In contrast, the glycolysis pathway appeared to be influenced by opposing enzymatic and allosteric regulations. These findings highlight key metabolic dysregulations that may contribute to the bioenergetic deficits in AD.

Introduction

Alzheimer's disease (AD) is a leading cause of dementia and affects tens of millions of people worldwide currently (Breijyeh & Karaman, 2020). It is pathologically characterized by senile plaques, neurofibrillary tangles, and cerebral atrophy (Breijyeh & Karaman, 2020). Many risk factors are involved in the development of this disease: aging, genetic factors, vascular disease, infections, environmental factors, and metabolic disorders (Scheltens et al., 2021). Among these hallmarks, some studies have focused on the role of altered metabolism in AD. One well-known abnormality that appears early in the progression of dementia is downregulation of glucose metabolism (Yan et al., 2020). In the clinical settings, fluorodeoxyglucose (FDG)-positron

emission tomography (PET) is used to detect the changes in glucose metabolism in brain and to distinguish between different types of dementia (de la Monte & Tong, 2014). FDG-PET detects reduced glucose consumption in the parietal-temporal area, medial temporal lobes, and posterior cingulate cortices during early AD, which later extends to the frontal lobes and subcortical areas (Mosconi et al., 2009; Szablewski, 2021). One of the causes for the dysregulation of glucose metabolism is the downregulation of GLUT1 and GLUT3, glucose transporters involved in glucose uptake into brain tissue. These transporters are downregulated in AD patients (Kyrtata et al., 2021; Liu et al., 2008; Simpson et al., 1994), correlating with the extent of amyloid beta (Aβ) accumulation and neurofibrillary tangles (An et al., 2018; Liu et al., 2008). Mitochondrial dysfunction is another key feature of AD pathology (Swerdlow, 2020). Studies of postmortem brain tissue have revealed impairments in the pyruvate dehydrogenase complex (PDHC) (Bubber et al., 2005; Parker et al., 1994) and mitochondrial respiratory chain complexes (Parker et al., 1994) in patients with AD compared to cognitively normal subjects. More recently, there has been growing interest in the link between type 2 diabetes mellitus and AD, because brain insulin resistance has been observed in AD brains. This pathology, defined as the failure of brain cells to respond to insulin, leads to synaptic dysfunction and impaired immune response (Arnold et al., 2018; Steen et al., 2005). Together, these metabolic abnormalities result in bioenergetic deficits, oxidative stress, chronic inflammation, and protein quality control failures in AD (Kumar et al., 2022).

Large-scale and multi-omic analyses have identified many genes, proteins, and metabolic pathways that are associated with AD (Beckmann et al., 2020; Leventhal et al., 2024; M. Wang et al., 2021). For example, co-expression network analysis of brain proteomic data has identified protein network modules associated with microglia, astrocytes, and sugar metabolism as the most strongly altered in AD (Johnson et al., 2020). Integrative multi-omic network analysis has shown that short-chain acylcarnitines/amino acids and medium/long-chain acylcarnitines are most associated with AD clinical outcomes, implicating regulatory roles of *ABCA1* and *CPT1A* (Horgusluoglu et al., 2022). More recently, machine learning techniques have been applied to the integration of multi-omic data and the identification of functional modules and key molecules related to AD (Moon & Lee, 2022; J. Wang et al., 2024). However, these studies predominantly focus on correlations-based analyses and biomarker discovery rather than elucidating the detailed mechanistic regulation by the physicochemical interactions among molecules across different modalities.

“Trans-omic analysis” can be a powerful approach for reconstructing a cross-hierarchical molecular regulatory network by integrating comprehensive quantitative data of molecules measured at multiple levels (gene expression level, protein abundance, and metabolite abundance) with existing molecular biological knowledge. Such an approach has been applied to study obesity in mouse models and identified regulatory changes in metabolic reactions in the liver and muscle in either the fasting state or after glucose administration in wild-type mice and *ob/ob* mice (Egami et al., 2021; Kokaji et al., 2022; Sugimoto et al., 2024).

Here, we reconstructed a trans-omic network to uncover regulatory changes in metabolic reactions between cognitively normal control subjects and AD patients. We used public multi-omic datasets (transcriptomic, proteomic, and metabolomic data) of the dorsolateral prefrontal cortex (DLPFC) from the Religious Order Study and the Memory and Aging Project (ROSMAP) study (Bennett et al., 2018, 2012). The metabolic trans-omic analysis revealed putative AD-associated dysfunction due to changes in enzyme abundance and allosteric regulation by metabolites in pathways related to energy production, including the glycolysis pathway, the TCA cycle, the oxidative phosphorylation pathway, and ketone body metabolism. Our study provides a systems-level insight into intracellular metabolic dysregulation that may underlie the pathology of AD.

Results

Overview of trans-omic analysis for metabolic reactions of Alzheimer's disease

To understand metabolic dysfunction in AD, we constructed a trans-omic network that integrated transcriptomic, proteomic, and metabolomic data from postmortem human brain tissue. We primarily used public multi-omic datasets (Batra et al., 2023; De Jager et al., 2018; Johnson et al., 2020) obtained from the DLPFC collected from cognitively normal individuals and patients with AD in the ROSMAP study (Bennett et al., 2018, 2012). Although pathological changes in AD are prominent in other brain areas, including temporal and parietal lobes, our study focused on the DLPFC due to the unique availability of comprehensive and matched multi-omic data for this region. The transcriptome was measured by bulk RNA sequencing (NGS), the proteome by tandem mass tag (TMT)-MS, and the metabolome by UPLC-MS/MS (Fig. 1).

We identified differentially expressed genes (DEGs), proteins (DEPs), and metabolites (DEMs) in patients with AD compared to cognitively normal controls using each omic dataset (Fig. 1, Step 1). To focus on metabolic regulation, we used KEGG (Kanehisa et al., 2025) and BRENDA (Chang et al., 2021) to match enzymes and metabolites to metabolic reactions and then determined AD-associated differences in metabolic regulation ("differential regulation") (Fig. 1, Step 2). We also identified the enzyme mRNAs and transcription factors (TFs) that may be involved in the metabolic changes in AD (Zou et al., 2024). We then reconstructed a metabolic trans-omic network through integrating all these molecular relationships spanning multi-omic modalities (Fig. 1, Step 3). We further analyzed key metabolic pathways in the trans-omic network related to energy production, including glycolysis, the TCA cycle, oxidative phosphorylation, and ketone body metabolism (Fig. 1, Step 4).

Identification of differentially expressed molecules of AD

We accessed the omic datasets and associated clinical, demographic, and postmortem neuropathological data for each individual from the ROSMAP study through the AD Knowledge Portal (*https://adknowledgeportal.synapse.org/*). A detailed summary of the samples used in this study, including the overlap across the three omicmodalities, is provided in Fig. S1. To ensure the representativeness of this cohort, we compared the ROSMAP study dataset with other public datasets (MSBB study and Wan et al., 2020 for transcriptomic validation; AMP-AD Diverse Cohorts for proteomic validation; Batra et al., 2024 and Novotny et al., 2023 for metabolomic validation), confirming significant correlations or overlap in AD-related changes across independent datasets (Fig. S2). Furthermore, to address potential alterations in the cell type proportions associated with AD, we identified overlapping individuals between our bulk omic datasets and a previously published single-nucleus transcriptomic dataset (Green et al., 2024). For the overlapping samples, we calculated major cell type proportions and statistically compared them between cognitively normal subjects and patients with AD (Fig. S3). In the transcriptomic data, we have confirmed significantly increased proportion of oligodendrocytes and decreased proportion of inhibitory neurons in patients with AD. In the metabolomic data, we found significantly decreased proportion of inhibitory neurons in patients with AD.

We defined the cognitively normal control (CT) group and the AD group based on clinical diagnosis and neuropathological diagnoses (Braak Stage and CERAD score) (see also Fig. S1A and Methods section) (Bennett et al., 2018, 2012). We defined 946 significantly increased mRNAs and 917 decreased mRNAs in AD using the results of the differential expression analysis from the RNA-seq Harmonization Study (Wan et al., 2020) (Synapse id: syn8456721). We identified 657 significantly increased proteins and 854 decreased proteins in AD using the proteomic data in the ROSMAP Study (id: syn21266454) (Johnson et al., 2020). We identified 79 significantly increased metabolites and 78 decreased metabolites in AD using the metabolomic data from the ROSMAP study (id: syn25985690) (Batra et al., 2023).

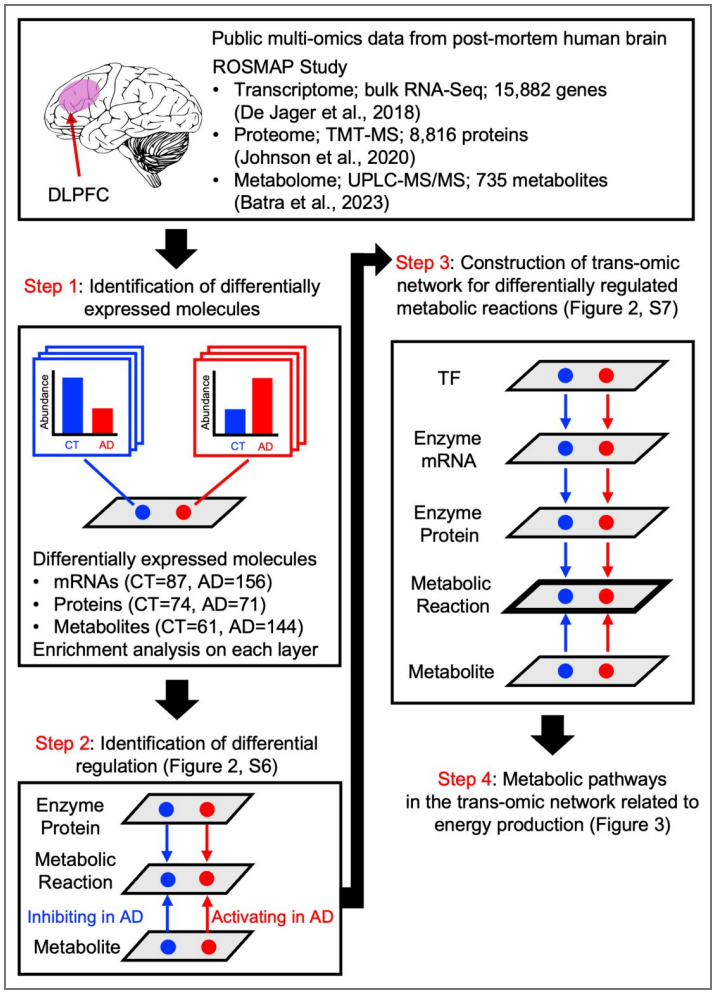

Figure 1. Overview of trans-omic analysis for metabolic reactions in Alzheimer's disease

The illustration shows how public multi-omic data from the DLPFC of cognitively normal subjects (CT) and patients with Alzheimer's disease (AD) from the ROSMAP study were used to generate a metabolic trans-omic network (Steps 1-3) and to perform detailed analysis of energy production pathways (Step 4). Red indicates differentially expressed molecules with increased expression or abundance, regulatory events that activate metabolic reactions, or increased activity of a metabolic reaction. Blue indicates differentially expressed molecules with decreased expression or abundance, regulatory events that inhibit metabolic reactions, or reduced activity of a metabolic reaction. The sample size for each analysis: n = 87 (CT group) and n = 156 (AD group) for transcriptomics, n = 74 (CT group) and n = 71 (AD group) for proteomics, and n = 61 (CT group) and n = 144 (AD group) for metabolomics.

Additionally, we conducted enrichment analyses for each omic dataset (Fig. S4D), highlighting upregulation of nitrogen metabolism and downregulation of ribosomal function. Furthermore, we constructed protein-protein interaction networks for the increased and decreased DEPs using the STRING database (Szklarczyk et al., 2023) (Fig. S5 and Supplementary Data 2). The result indicated downregulated translation, both in the nucleus and in the mitochondria. We also visualized the top 20 DEGs, DEPs, and DEMs with $\log_2$FC values (Fig. S6 and Supplementary text). Of note, the abundance of ATP was not quantified in the metabolomic data from the ROSMAP study (Batra et al., 2023).

Relationship between proteomic changes and gene expression changes in AD

To examine the relationship between DEGs and DEPs, we investigated the expression changes of the genes encoding each DEP (Fig. S7A). Among the increased DEPs, 76 DEPs were encoded by significantly upregulated genes, and 15 DEPs were encoded by significantly downregulated genes. Among the decreased DEPs, 70 DEPs were encoded by genes with significantly decreased expression, and 12 DEPs were encoded by genes with significantly increased expression. Thus, many of the DEPs did not have coordinated expression changes with their encoding genes (Fig. S7B). This result is consistent with previous studies using postmortem human transcriptomic and proteomic data (Johnson et al., 2022; Tasaki et al., 2022).

Identification of differentially expressed transcription factors

We identified TFs potentially involved in regulating the expression changes of the DEGs using ChIP-Atlas, a database that integrates and provides ChIP-seq data (Zou et al., 2024). No TFs were predicted to regulate genes with significantly decreased expression; 19 TFs were identified as regulators of genes with significantly increased expression (Table S1). To determine the TFs with differential activity in AD, we investigated whether the predicted TFs were encoded by DEGs or were DEPs (Fig. S7C). We identified five TFs that were significantly increased at either the transcriptomic level (CTCF, MAX, and ZNF143) or the proteomic level (BRD4 and RAD21). We defined these 5 TFs as “differentially expressed transcription factors” (DETFs). Recent findings have shown the protective role of BRD4, which inhibits transcriptional expression of AD-risk genes (Matuszewska et al., 2022; Nikkar et al., 2022; Sun et al., 2024).

Identification of metabolic enzymes among the differentially expressed proteins

To focus on the proteomic changes in AD that are relevant to cellular metabolism, we identified metabolic enzymes among the DEPs according to their designations as metabolic enzymes in the “Metabolic pathways” of the KEGG PATHWAY Database (Kanehisa et al., 2025). Among the 657 significantly increased proteins, 59 are metabolic enzymes. Among the 854 significantly decreased proteins, 70 are metabolic enzymes (Table S2).

Identification of metabolites that are substrates, products, or allosteric regulators of metabolic reactions

Metabolic reactions are regulated not only by the abundance of the metabolic enzymes that catalyze the reactions, but also by the abundance of substrates and products, as well as by allosteric regulators. Using the BRENDA database (Chang et al., 2021), we identified allosteric regulators among the DEMs: 46 were increased in AD and 26 were decreased in AD (Fig. 2A). These 72 allosteric regulatory DEMs affected 318 enzymes. Using the KEGG REACTION database (Kanehisa et al., 2025), we also identified substrates and products of metabolic reactions among the DEMs: 50 substrates or products were increased in AD and 33 were decreased in AD, affecting 727 enzymes (Fig. 2B).

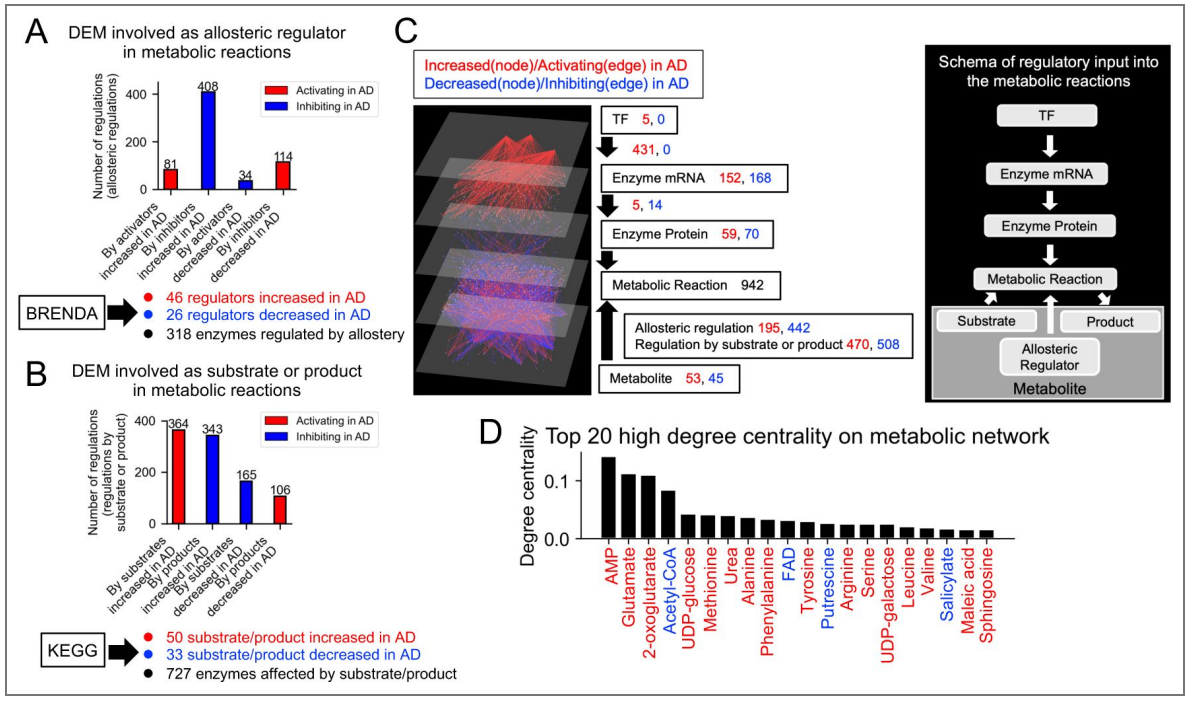

Figure 2. Construction of a trans-omic network for differentially regulated metabolic reactions

(A) The number of allosteric regulators among DEMs and the number of allosteric regulations mediated by them on metabolic enzymes identified with BRENDA. Some reactions are regulated by more than one DEM and some DEMs regulate multiple enzymes, thus the number of regulations exceeds the number of enzymes identified with BRENDA and the number of DEMs. (B) The number of substrates or products among DEMs and the number of regulations by them on metabolic enzymes identified with KEGG. Some reactions involve multiple substrates or yield multiple products and some substrates and products occur in multiple reactions, thus the number of regulations exceeds the number of enzymes identified with KEGG and the number of DEMs. (C) The trans-omic network for differentially regulated metabolic reactions (left). Nodes and edges indicate differentially expressed molecules and differential regulations involved in metabolic reactions, respectively. Schema of regulatory input into the metabolic reactions (right). TFs control metabolic enzyme mRNA abundance through gene regulation. Metabolite acts as substrates, products, and allosteric regulators in metabolic reactions. See Fig. S8 and Methods section for additional details. (D) Top 20 molecules with high degree centrality on the metabolic network. The metabolic network consisted of the nodes and edges from the “Enzyme Protein”, “Metabolic Reaction”, and “Metabolite” layers of the trans-omic network. Those shown in red text were increased in AD; those in blue were decreased in AD.

Construction of a trans-omic network for differentially regulated metabolic reactions

We constructed a metabolic trans-omic network for differentially regulated metabolic reactions in AD (Fig. 2C and Supplementary Data 1). This network integrates five interconnected components organized into corresponding layers: (1) DETFs in the "TF layer", (2) DEGs encoding metabolic enzymes in the "Enzyme mRNA layer", (3) DEPs functioning as metabolic enzymes in the "Enzyme Protein layer", (4) metabolic reactions differentially regulated by enzymes or metabolites in the "Metabolic Reaction layer", and (5) DEMs involved in the metabolic reactions as allosteric regulators, products, or substrates in the "'Metabolite layer". The adjacent layers are connected by edges based on the regulatory relationships between the molecules. The right panel of Fig. 2C shows the schema for the construction of the trans-omic network, corresponding to the five layers in the left panel. Specifically, the interlayer connections from the "Metabolite layer" to the "Metabolic Reaction layer" consisted of regulatory connections mediated by allosteric regulators, substrates, or products of each metabolic reaction (Egami et al., 2021; Kokaji et al., 2022). Activating regulation of metabolic reactions is shown as red edges, and inhibiting regulation is shown as blue edges (see also Fig. S8, and Methods section).

We analyzed the degree centrality of nodes in the metabolic reaction network that consisted of "Enzyme Protein layer", "Metabolic Reaction layer", and "Metabolite layer." Degree centrality is a measure of the importance of a node in network theory (Koschützki & Schreiber, 2008). The degree centrality of a node is calculated by normalizing the number of edges connected to that node, with a higher value indicating greater influence within the network. AMP, which increased in the AD group, had the highest degree centrality (Fig. 2D). Glutamate, 2-oxoglutarate (α-ketoglutarate), and urea, which were increased in AD, were second, third, and seventh in degree centrality, respectively. Acetyl-CoA, which decreased in the AD group, ranked fourth.

The metabolic dysregulations of energy metabolic pathways of AD

We extracted key metabolic pathways involved in energy production in the trans-omic network, the glycolysis pathway, the TCA cycle, oxidative phosphorylation, and ketone body metabolism. We examined detailed metabolic dysregulation in each pathway (Fig. 3).

In the glycolysis pathway, increased expression of TPI1, GAPDH, PGAM2, ENO1, and PKM would increase flux through the glycolysis pathway, whereas the increased metabolites S7P, AMP, threonine, alanine, tyrosine, valine, urea, glutamate, and phenylalanine would allosterically inhibit flux through the pathway. In addition, the expression of GLUT3, a transporter responsible for the basal uptake of glucose in neurons (Koepsell, 2020), is significantly decreased (Fig. 3A), as demonstrated in several previous studies (An et al., 2018; Liu et al., 2008; Simpson et al., 1994). However, the mRNA expression of *GLUT3* did not show a significant change in AD in the transcriptomic dataset we used.

Previous studies have reported downregulation of PDHC in AD patients (Jankowska-Kulawy et al., 2022; Jia et al., 2023). Consistently, we found that five of the six proteins comprising the complex, PDHA1, PDHB, PDHX, DLD and DLAT, were significantly decreased. In addition, acetyl-CoA, was significantly decreased in AD. The previous studies (Jankowska-Kulawy et al., 2022; Jia et al., 2023) and our findings suggest that reduced PDHC activity may decrease the production of acetyl-CoA in AD.

In the TCA cycle, most regulations were inhibitory (Fig. 3B). Three metabolic enzymes were significantly decreased: SDHA, CS, and IDH2. Increases in AMP, glutamate, and maleic acid resulted in allosteric inhibition of metabolic reactions in the TCA cycle. Only a reduction in nicotinamide D-ribonucleotide exhibited an allosteric activating effect. Among the five measured metabolites (citrate, aconitate, 2-oxoglutarate, fumarate, and malate) that are substrates and products in the TCA cycle, 2-oxoglutarate (α-ketoglutarate) showed a significant increase in abundance.

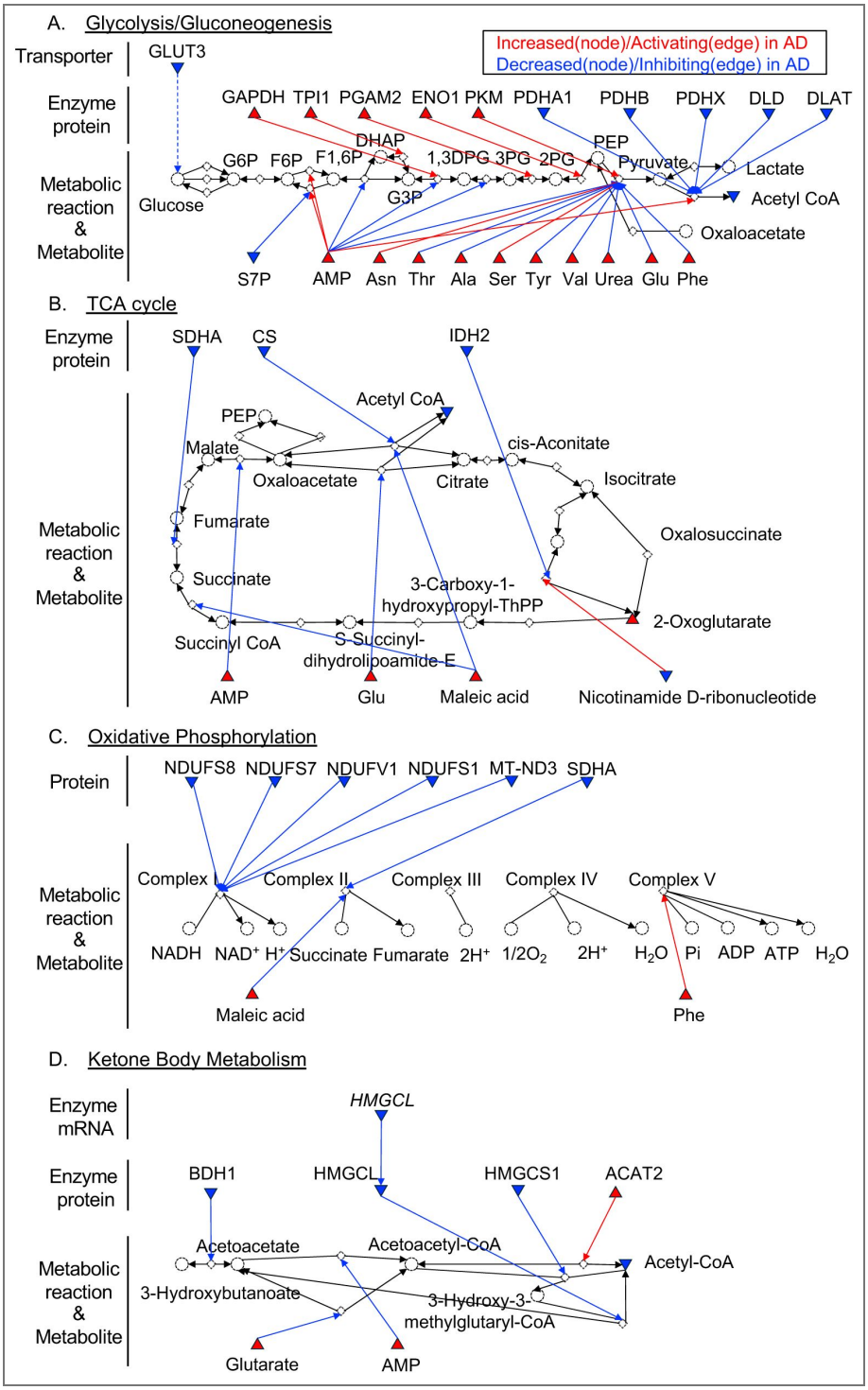

Figure 3. The metabolic dysregulations of energy metabolic pathways of AD

The trans-omic changes in the regulations of glycolysis (A), TCA cycle (B), oxidative phosphorylation (C), and ketone body metabolism (D). The information for each pathway were obtained from "glycolysis/gluconeogenesis" (hsa00010), "TCA cycle" (hsa00020), "oxidative phosphorylation" (hsa00190), and "butanoate metabolism" (hsa00650) in the KEGG database. Red upward triangles, increased molecules in AD; blue downward triangles, decreased molecules in AD. Red arrow, regulations that activate metabolic reactions; blue arrow, regulations that inhibit reactions. Unfilled circles with dashed outlines represent molecules that were not differentially expressed or were not measured. Unfilled diamond nodes with dashed outlines represent metabolic reactions. See Fig. S8 and Methods section for additional details.

In oxidative phosphorylation, most of the regulatory changes in AD resulted in inhibition of metabolic reactions (Fig. 3C). Five subunits of complex I in the respiratory chain were decreased: NDUFS8, NDUFS7, NDUFV1, NDUFS1, and MT-ND3. This result is consistent with other postmortem studies of human brains which have shown reduced expression of genes encoding subunits of the electron transport chain in posterior cingulate cortex, middle temporal gyrus, and the hippocampus of AD patients (Liang et al., 2008). The activity of complex II was also negatively impacted by the decrease in SDHA and an increase in the allosteric inhibitor, maleic acid. The increase in phenylalanine, an allosteric regulator of complex V, provided the only activating regulation.

Ketone bodies are the second-most utilized energy source in the brain after glucose (Jensen et al., 2020). Ketone bodies are synthesized in the liver in the form of 3-hydroxybutyrate and acetoacetate, which are transported to the brain through the circulation (Jensen et al., 2020). Ketone bodies undergo several metabolic reactions and are converted to acetyl-CoA as an energy source in mitochondria (Jensen et al., 2020). Most of the AD-associated changes resulted in inhibition of ketone body metabolism (Fig. 3D). Among the metabolic enzymes involved in ketone body metabolism, BDH1, HMGCL, and HMGCS1 were downregulated; only ACAT2 was upregulated. The increase in glutarate and AMP resulted in inhibitory allosteric regulation. Collectively, these results suggested that reduced ketone body metabolism contributed to the decrease in acetyl-CoA abundance in AD.

Through this examination of the changes in the regulation of core metabolic pathways involved in energy production, we found putative antagonistic regulation by enzymes and allosteric regulators in the glycolysis pathway. On the other hand, the TCA cycle, oxidative phosphorylation, and ketone body metabolism can be downregulated in AD due to the reduced enzymes and inhibitory allosteric effects. Here, we demonstrate the systems-level view of the potential dysregulated energy production of AD in terms of the metabolic trans-omic network.

Discussion

In this study, we identified differentially expressed molecules from public datasets of transcriptome, proteome, and metabolome obtained from the ROSMAP study and used the results to construct a metabolic trans-omic network in AD. We then performed a detailed analysis of the AD-associated changes in pathways related to energy production. Above all, we summarized the metabolic dysregulations observed in the brain of AD (Fig. 4).

Several key factors that underlie the mechanism of dysregulated energy metabolism have been identified in many previous studies (An et al., 2018; Arnold et al., 2018; Bubber et al., 2005; Kyrtata et al., 2021; Liu et al., 2008; Parker et al., 1994; Simpson et al., 1994; Steen et al., 2005; Swerdlow, 2020; Yan et al., 2020), including downregulated glucose uptake and utilization, impaired mitochondrial functions, dysfunctional enzyme proteins, and brain insulin resistance, among others. However, details of the regulatory relationships between the molecules belonging to different modalities have been poorly understood. Here, we demonstrated a potential mechanistic picture of dysregulated core energy metabolism in AD (Fig. 4): (1) inhibition of the TCA cycle, oxidative phosphorylation, and ketone body metabolism by allosteric inhibition and downregulated enzyme proteins, (2) antagonistic regulation by enzymes and allosteric regulators in the glycolysis pathway.

As previously reported (Yu et al., 2022), mitochondrial dysfunction accompanies the progression of AD, which may lead to downregulation of TCA cycle, oxidative phosphorylation, and ketone body utilization pathways, as we confirmed in this study, since these metabolic reactions occur within mitochondria. Additionally, decreased expression of the subunit proteins that make up PDHC and allosteric inhibition to the glycolysis pathway may further reduce acetyl-CoA levels, resulting in a greater decrease in the ability to produce enough ATP. This energetic shortage appears to be partially compensated by upregulation of glycolytic enzymes, but this compensatory mechanism could be inhibited by the reduced glucose uptake through GLUT3 in neurons. This

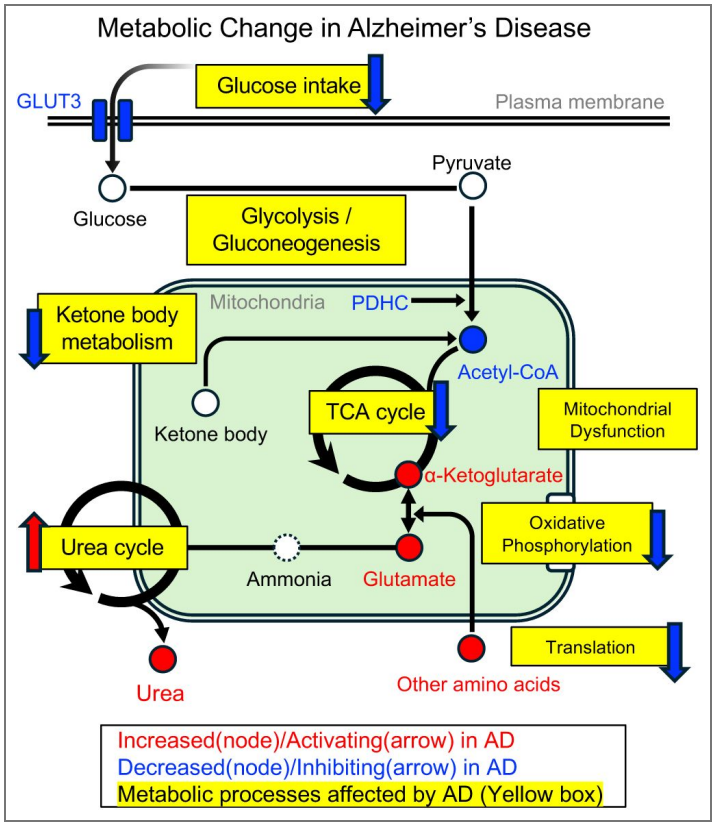

Figure 4. Models of potentially dysregulated metabolic processes in AD

Diagrams of dysregulated metabolic pathways associated with the progression of AD. Metabolic processes affected by AD are highlighted in yellow boxes. Red, increased (circles) or activating (arrows) in AD; blue, decreased (circles and GLUT3) or inhibiting (arrows) in AD.

hypothesis is supported by the previous study, which has suggested an upregulated glycolysis pathway in astrocytes as a compensatory mechanism to provide the energy source for impaired neurons during AD progression (Fu et al., 2015).

The DEM analysis revealed significant increases in 12 amino acids (Glu, Tyr, Thr, Phe, Asn, Ser, Arg, Val, Leu, Ala, Met, and Lys), 2-oxoglutarate, and urea. In addition, we identified ASL, an enzyme involved in the urea cycle (Hansmannel et al., 2010), as significantly increased in AD. Thus, our results highlighted the potential involvement of nitrogen metabolism dysregulation in AD and suggested that the observed accumulation of urea may result from enhanced flux through the urea cycle within the DLPFC. This could reflect a response to elevated amino acid levels, potentially linked to compromised translation and protein turnover. This hypothesis is also supported by the results of our PPI network analysis and the low correlation between mRNA expression and protein expression.

Previous studies have demonstrated that transcripts of ribosomal proteins are significantly decreased in the dentate gyrus in AD patients (Hernández-Ortega et al., 2016). In another recent research, changes in the proteome are important for understanding AD pathology, because approximately half of the network modules identified in protein networks were not found in RNA networks (Johnson et al., 2022). About nitrogen metabolism in AD, a previous study has demonstrated that astrocytic urea metabolism induced in AD has a beneficial effect on Aβ detoxification. However, this metabolic process has been found to induce memory impairment through producing toxic byproducts, ammonia and H_2O_2, and GABA (Ju et al., 2022).

Limitations of this study

Several methodological limitations of our study should be acknowledged. Our analysis did not distinguish between cell types. Brain tissue contains various types of cells: neurons, astrocytes, oligodendrocytes, and microglia. The genes and proteins expressed in each cell type differ, as do the metabolic reactions that occur within each cell (Bonvento & Bolaños, 2021; Magistretti & Allaman, 2015). We primarily observed a decreased proportion of inhibitory neurons in the transcriptomic and metabolomic datasets (Fig. S3A and S3C). Additionally, previous studies has reported that Braak stage negatively correlated with the proportion of oligodendrocytes and positively correlated with the proportions of microglia and astrocytes (Hannon et al., 2024; Shireby et al., 2022). Therefore, our results could partly reflect changes in tissue composition associated with the progression of AD. A recent study using the snRNA-seq technique has demonstrated that in excitatory neurons downregulated DEGs that were correlated with NFT burden were enriched for TCA cycle (Mathys et al., 2024). In addition, the glycolysis and oxidative phosphorylation modules were upregulated in astrocytes and microglia in AD group (Mathys et al., 2024).

All omics data used in this study were measured from postmortem brain tissues. The cause of death and events that occur immediately before death (such as resuscitation) can influence molecular profiles of postmortem tissue. Thus, we must consider potential biases related to these factors. In addition, post-mortem interval (PMI) can affect the results of the quantifications of molecules. Regarding the metabolomic dataset that we used, about 300 metabolites were found to be associated with PMI in the original research (Batra et al., 2023). Thus, we included PMI as a covariate in the differentially expressed analysis.

In this study, we analyzed the DLPFC because that was the region with sufficient datasets. However, initial pathological changes of AD typically appear in the medial temporal lobe. Therefore, trans-omic analyses should also be conducted in this region. It is also possible that the results of this study reflect changes that compensate for metabolic alterations arising in other regions. However, at present, the number of large-scale proteomic and metabolomic datasets measured from human postmortem brains is limited.

Interpretation of regulatory relationships among altered molecules within the trans-omic network remains challenging because they are often highly complex and densely interconnected. For example, lipid metabolism is widely recognized as playing a critical role in AD pathology (Baloni et

al., 2020; Horgusluoglu et al., 2022; Varma et al., 2021). However, our analytical framework did not allow for a sufficiently detailed dissection of lipid metabolic dysregulation. In addition, the trans-omic network analysis is sensitive to predefined analytical settings, including statistical thresholds for defining differentially expressed molecules and sample size. Therefore, our findings should be interpreted as an observational systems-level insights rather than definitive mechanistic conclusions into AD pathology. Further verification using independent and larger cohorts, as well as experimental validation will be essential in future studies.

Materials & methods

ROSMAP study

Public multi-omic datasets measured from postmortem human brain samples from the Religious Orders Study and Memory and Aging Project (ROSMAP) study were primarily used in this study. (*https://adknowledgeportal.synapse.org/Explore/Studies/DetailsPage/StudyDetails?Study=syn3219045#StudyDescription*) (Bennett et al., 2018, 2012). All data were obtained through the AD Knowledge Portal (*https://adknowledgeportal.synapse.org/*). The Religious Orders Study (ROS) and the Memory and Aging Project (MAP) are long-term studies that focus on memory, motor function, and functional problems in older adults. ROS includes Catholic nuns, priests, and brothers aged 65 and older; MAP includes older adults around Chicago. Both studies include annual clinical assessments, self-reports, and postmortem brain donations. Diagnosis of dementia is made using the same procedure in both studies, and final clinical diagnosis and pathological assessment are made after death. Further details of the studies can be found in (Bennett et al., 2018, 2012).

RNA sequencing

For transcriptomic data, the results of differential expression analysis from the RNAseq Harmonization Study (De Jager et al., 2018) were used. For detailed methods of RNA-seq and differential expression analysis, see (*https://adknowledgeportal.synapse.org/Explore/Studies/DetailsPage/StudyDetails?Study=syn3219045#Methods-GeneExpressionRNAseq*) and (*https://adknowledgeportal.synapse.org/Explore/Studies/DetailsPage/StudyDetails?Study=syn9702085#StudyDescription*).

Proteomic analysis

For the proteomic data, proteomic analysis in the ROSMAP study was used (Johnson et al., 2020). In that study, brain tissue samples from the ROSMAP cohort (n = 400) were tagged using the TMT 10-plex kit. Further details of the TMT-MS experiment are available at (*https://adknowledgeportal.synapse.org/Explore/Studies/DetailsPage/StudyDetails?Study=syn3219045#Methods-ProteomicsTMTquantitation*). For information on batch effect correction, outlier and covariate adjustment of the raw data, refer to (Johnson et al., 2020).

Metabolomic analysis

For metabolomic data, UPLC-MS/MS analysis in the ROSMAP Study was used, which were generated at Metabolon and preprocessed by the Alzheimer's Disease Metabolomics Consortium (Batra et al., 2023). Further details of the UPLC-MS/MS experiments and data normalization can be found at (*https://adknowledgeportal.synapse.org/Explore/Studies/DetailsPage/StudyDetails?Stud* y=syn3219045#Methods-MetabolomicsMetabolonHD4).

Validation analysis

To ascertain how the choice of the ROSMAP Study as the data source could influence our analyses, the ROSMAP Study data were compared with other datasets or findings from specific published studies (Fig. S2). For transcriptomic validation, RNA-seq data from the Mount Sinai Brain Bank (MSBB) study (*https://www.synapse.org/Synapse:syn10526259*) were used. Log_2 fold-change

values were calculated for each gene by taking the $\log_2$ ratio of the mean expression in the AD group to that in the CT group, and Pearson correlation coefficients were calculated between the two datasets (Fig. S2A). In addition, we compared our ROSMAP-derived DEGs with those identified in a large-scale meta-analysis of 2,114 samples across seven brain regions using a fixed-effects model (q-value < 0.05) (Wan et al., 2020) (Fig. S2B, C). For validation of proteomic data, TMT-MS results from the Accelerating Medicines Partnership Alzheimer's Disease Diverse Cohorts Study (AMP-AD DiverseCohorts) were used (*https://www.synapse.org/Synapse:syn55249985*) (Reddy et al., 2024).

Correlation analysis was performed as described above (Fig. S2D). We additionally calculated a separate correlation coefficient for the subset of metabolic enzymes involved in the energy metabolism analysis shown in Fig. 3. To assess concordance in a threshold-independent manner, we performed rank-rank hypergeometric overlap (RRHO) analysis (Cahill et al., 2018; Plaisier et al., 2010) (Fig. S2E). For RRHO, proteins were ranked by $-\log_{10}$(q-value or p-value) multiplied by the sign of the $\log_2$ fold-change calculated in each study. For metabolomic validation, we compared our results with previous studies (Maffioli et al., 2022; Paglia et al., 2016; Xu et al., 2016) (Fig. S2F) and previous metabolomic datasets measured by UPLC-MS/MS platform (Batra et al., 2024; Novotny et al., 2023). RRHO analyses were performed to evaluate concordance in ranked metabolite changes as described above (Fig. S2G).

Cell type proportions analysis

A public single-nucleus transcriptomic dataset (Green et al., 2024) (id: syn31512863), which was obtained from DLPFC tissue of 465 subjects in the ROSMAP cohort, was used to assess the changes in cell type proportions associated with AD. For each omic data used in our analyses, we identified overlapping subjects and calculated the following cell type proportions for the matched samples: astrocytes, excitatory neurons, inhibitory neurons, microglia, oligodendrocytes, and OPCs. We statistically compared cell type proportions between control subjects and patients with AD using a two-tailed t-test, with the significance threshold set at p-value < 8.3×10^{-3} (Bonferroni correction).

Definition of CT group and AD group

The CT group consisted of subjects whose clinical diagnosis was categorized as "No cognitive impairment", with a Braak Stage of III or lower and a CERAD score indicating "no AD" or "possible AD". The AD group comprised subjects whose clinical diagnosis was categorized as "Alzheimer's dementia and no other cause of cognitive impairment", with a Braak Stage of IV or higher and a CERAD score indicating "probable AD" or "definite AD".

Identification of differentially expressed molecules between CT and AD

To define the differentially expressed genes (DEGs) in AD compared to CT, the results of the differential expression analysis from the RNA-seq Harmonization Study were used (*https://www.synapse.org/Synapse:syn8456721*). In the study, the adjusted p-value and log2FC value of each gene in the two groups were calculated using the count data from RNA sequencing of postmortem brains (DLPFC) from 634 subjects (156 AD and 87 CT) in the ROSMAP Study. The values were calculated after adjusting for covariates such as age, gender, post-mortem interval (PMI), and RNA integrity number (RIN) score using the voom-limma package in R. In that analysis, genes with an adjusted p-value < 0.05 were defined as DEGs.

To identify the DEPs in AD compared to CT, the log2-transformed and normalized relative quantitative data (*https://www.synapse.org/Synapse:syn21266454*) measured by isobaric tandem mass tagging peptide labeling in the ROSMAP study (71 AD and 74 CT) were used. Following the exclusion of proteins with more than 50% missing values, ANCOVA was performed with gender and PMI as covariates for the remaining 8,816 proteins. Subsequently, the q-value and log2FC were calculated using the Storey's method. Proteins with a q-value < 0.05 were defined as DEPs.

To identify the DEMs in AD compared to CT, the normalized quantified data (*https://www.synapse.org/Synapse:syn25985690*) measured using UPLC-MS/MS in the ROSMAP Study (144 AD and 61 CT) were used. Following the exclusion of metabolites with more than 50% missing values, ANCOVA was performed with gender and PMI as covariates for the remaining 735 metabolites. Subsequently, the q-value and log2FC were calculated using the Storey's method. Metabolites with q-values < 0.05 were defined as DEMs.

Enrichment analysis

Enrichment analyses were conducted on DEGs and DEPs using Metascape (version 3.5; *https://metascape.org/gp/index.html#/main/step1*) (Zhou et al., 2019). Enrichment analysis was conducted on DEMs using MetaboAnalyst (version 6.0; *https://www.metaboanalyst.ca/*) (Pang et al., 2024). The background was defined as all measured proteins for proteomic analysis, and all measured metabolites for metabolomic analysis.

Inference of transcription factors for differentially expressed genes in DLPFC of AD

To infer the TFs involved in regulating the DEGs, we used the peak call data (TSS±1k) from ChIP-Atlas (*https://chip-atlas.org/*) (Zou et al., 2024). The "neural" cell type was selected, and a threshold of 200 was applied for the statistical significance calculated by MACS2. The p-value was calculated using Fisher's exact test, and the Benjamini-Hochberg (BH) method was employed for FDR correction (q-value < 0.05).

Construction of protein-protein interaction networks

In constructing the protein-protein interaction network (Fig. S4A, S4B), we included protein pairs with a score of 400 or more in the STRING data (Szklarczyk et al., 2023) as interacting pairs. We constructed the protein-protein interaction network by connecting interacting DEPs with edges.

Construction of trans-omic network for differentially regulated metabolic reactions

DEPs and transcripts were matched using the Ensembl protein ID (Martin et al., 2023). Among the DEPs, proteins that were categorized as metabolic enzymes in the "metabolic pathways" of the KEGG PATHWAY database (Kanehisa et al., 2025) were identified. Using BRENDA (Chang et al., 2021), the allosteric regulators belonging to DEMs were identified. Using KEGG REACTION data, the DEMs that are involved as substrates or products in metabolic reactions were identified. By integrating the above information, we identified DEPs that act as metabolic enzymes, the metabolic reactions in which they are involved, and the DEGs encoding these proteins, as well as DEMs and the metabolic reactions in which these metabolites are involved as allosteric regulators or as products or substrates. To identify DETFs in AD, we examined which the inferred TFs were encoded by DEGs or appeared as the DEPs. All these data were used to construct a 5-layered (DETFs, DEGs, DEPs, metabolic reactions, DEMs) trans-omic network for metabolic reactions in the DLPFC of AD patients.

The adjacent layers are connected by edges based on the regulatory relationships between the molecules on these layers. The "Enzyme mRNA" and "TF" layers were connected by red edges when mRNA expression increased and by blue edges when it decreased. The "Enzyme mRNA" and "Enzyme Protein" layers were connected by red edges when both gene and protein expression of enzymes increased, and by blue edges when gene and protein expression of enzymes decreased. The "Enzyme Protein" and "Metabolic Reaction" layers were connected by red edges when enzyme expression increased, and by blue edges when enzyme expression decreased. For the connection between "Metabolic Reaction" and "Metabolite" layer, if a metabolite shows an increase in expression and also has an allosteric effect of activating the metabolic reaction it controls, it is colored red; if it shows an increase in expression and also has an allosteric effect of inhibiting the

metabolic reaction it controls, it is colored blue; if it shows a decrease in expression and also has an allosteric effect of activating the metabolic reaction it controls, it is colored blue; if it shows a decrease in expression and also has an allosteric effect of inhibiting the metabolic reaction it controls, it is colored red. If a metabolite shows an increase in expression and it is a substrate of the metabolic reaction, it is colored red; if it shows an increase in expression and it is a product of the metabolic reaction, it is colored blue; if it shows a decrease in expression and it is a substrate of the metabolic reaction, it is colored blue; if it shows a decrease in expression and it is a product of the metabolic reaction, it is colored red.

Implementation

Statistical tests were performed using MATLAB 2023b (The Mathworks Inc; *https://www.mathworks.com/products/matlab.html*). Trans-omic network analysis and visualization were implemented in Python (version 3.12.2; *https://www.python.org/*), Pandas (version 1.5.3; *https://pandas.pydata.org/*), Networkx (version 3.1; *https://networkx.org/*), and Matplotlib (version 3.7.1; *https://matplotlib.org/*) packages.

Resource availability

Lead contact

Further information and requests for resources and reagents should be directed to and will be fulfilled by the Lead Contact, Shinya Kuroda (*skuroda@bs.s.u-tokyo.ac.jp*).

Materials availability

This study did not generate any new material.

Supplementary

Supplementary figures

A

Item		Transcriptome		Proteome		Metabolome	
		AD	CT	AD	CT	AD	CT
Total subjects		156	87	71	74	144	61
Sex	male	46	39	14	28	35	26
	female	110	48	57	46	109	35
ApoE genotype	22	0	2	0	3	0	2
	23	9	14	4	15	10	11
	24	4	1	2	1	2	1
	33	82	62	49	50	75	42
	34	59	7	16	5	54	4
	44	2	1	0	0	3	1
Braak stage	0		5		3		4
	I		26		17		11
	II		14		14		13
	III		42		40		33
	IV	61		27		46	
	V	88		41		88	
	VI	7		3		10	
CERAD score	No AD		64		52		47
	Possible		23		22		14
	Probable	57		26		59	
	Definite	99		45		85	
Age at death	65~70	0	1	0	0	0	0
	70~75	1	7	0	2	0	2
	75~80	4	17	0	13	3	7
	80~85	15	19	4	17	12	11
	85~90	51	27	18	21	34	17
	Over 90	85	16	49	21	95	24
Postmortem interval (hours)	0~5	52	26	15	18	27	13
	5~10	74	45	43	42	94	39
	10~15	16	9	5	8	13	3
	15~20	11	6	4	2	7	3
	20~25	3	0	3	4	2	3
	25~30	0	1	0	0	0	0
	30~35	0	0	1	0	1	0

B

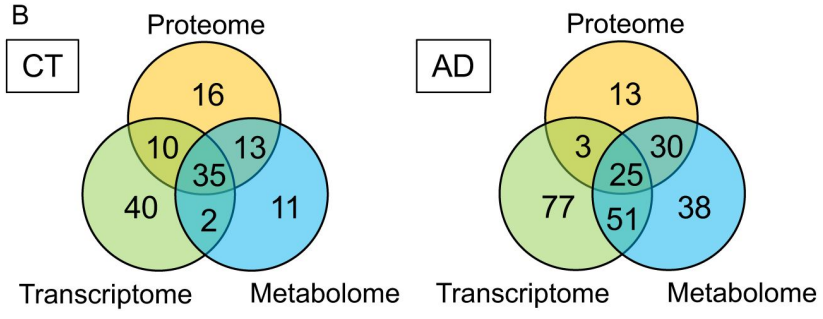

Figure S1. Information for the subjects from ROSMAP study. (A) Information of the samples from ROSMAP Study used in this study, including sample size, sex, ApoE genotype, Braak Stage, CERAD score, age at death, and

postmortem interval (PMI). (B) Venn diagrams showing the overlap in data available for each subject across the three omic levels: transcriptome, proteome, and metabolome.

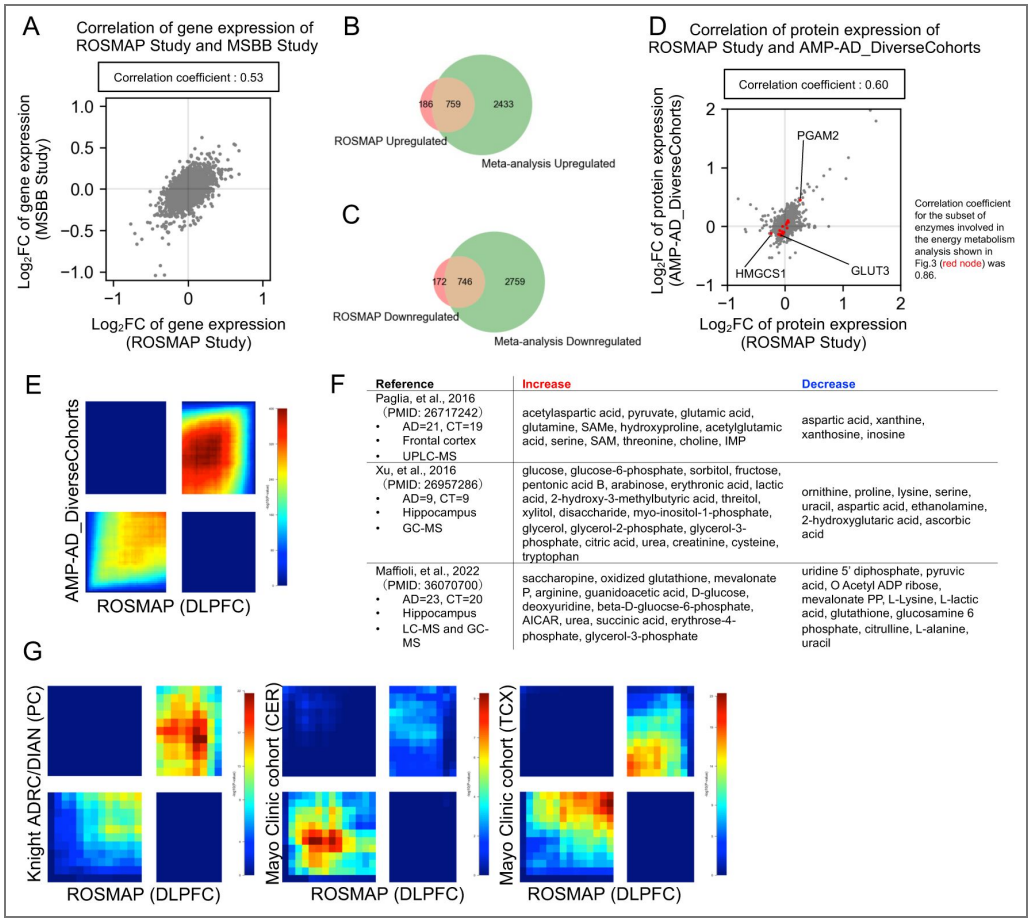

Figure S2. Comparison of transcriptome, proteome, and metabolome data from the ROSMAP Study with data from other studies.

(A) Correlation between two transcriptomic datasets obtained from the ROSMAP Study and the MSSB Study for each gene. In the MSSB Study, RNA sequencing data were collected from brain tissue (FP; frontal pole) of individuals with AD (45 AD patients) and control subjects (45 CT subjects). For correlation analysis, the $\log_2$ fold-change values in 16,348 genes were calculated by dividing the average expression of the AD group by the average expression of the CT group. (B) Venn diagrams showing the overlap of upregulated DEGs between the ROSMAP study and those identified in a large-scale meta-analysis across seven brain regions [81]. (C) Venn diagrams showing the overlap of downregulated DEGs between the ROSMAP study and those identified in a large-scale meta-analysis across seven brain region [81]. (D) Correlation between two proteomic datasets obtained from the ROSMAP study and AMP-AD_DiverseCohorts study for each protein. TMT-MS data from each study were from brain tissue (DLPFC) of individuals with AD (637 AD patients) and control subjects (224 CT subjects). Correlation analysis was performed on the $\log_2$ fold-change values (average abundance of AD divided by average abundance of CT) for 9,180 proteins. Specifically, red nodes represent the subset of enzyme proteins which are involved in energy metabolism shown in Fig.3. (E) Rank-rank hypergeometric overlap (RRHO) heatmap comparing proteomic changes in AD compared to CT between the ROSMAP study (x-axis) and the AMP-AD_DiverseCohorts study (y-axis). Proteins were ranked based on $-\log_{10}$(q-value) multiplied by the sign of $\log_2$ fold-change in each dataset. Color intensity represents $-\log_{10}$(p-value) of the overlap at each rank threshold. Enrichment in bottom-left and top-right quadrants indicates concordant changes between the two datasets. (F) Differentially expressed metabolites (DEMs) identified in previous studies [71,72,73]. Note that each study used different definitions for AD and CT groups, had variations in measurement methods and brain regions analyzed. These studies had smaller sample sizes than our study. (G) RRHO heatmaps comparing metabolite changes in AD compared to CT between the ROSMAP study (DLPFC) (x-axis) and independent metabolomic datasets from multiple cohorts and brain regions [82,83] (y-axis). The Knight ADRC/DIAN dataset [83] consisted of 79 postmortem brain samples from cerebellar cortex (CER) of AD, 24 samples from CER of CT, 63 samples from temporal cortex (TCX) of AD, and 20 samples from TCX of CT and quantified 627 metabolites. The Mayo Clinic cohort datasets [82] consisted of 305 postmortem brain samples from parietal cortex (PC) of AD, 26 samples from PC of CT and quantified 685 metabolites. Metabolites were ranked based on $-\log_{10}$(p-value or q-value) multiplied by the sign of $\log_2$ fold-change in each dataset. Enrichment in bottom-left and top-right quadrants indicates concordant changes between the two datasets.

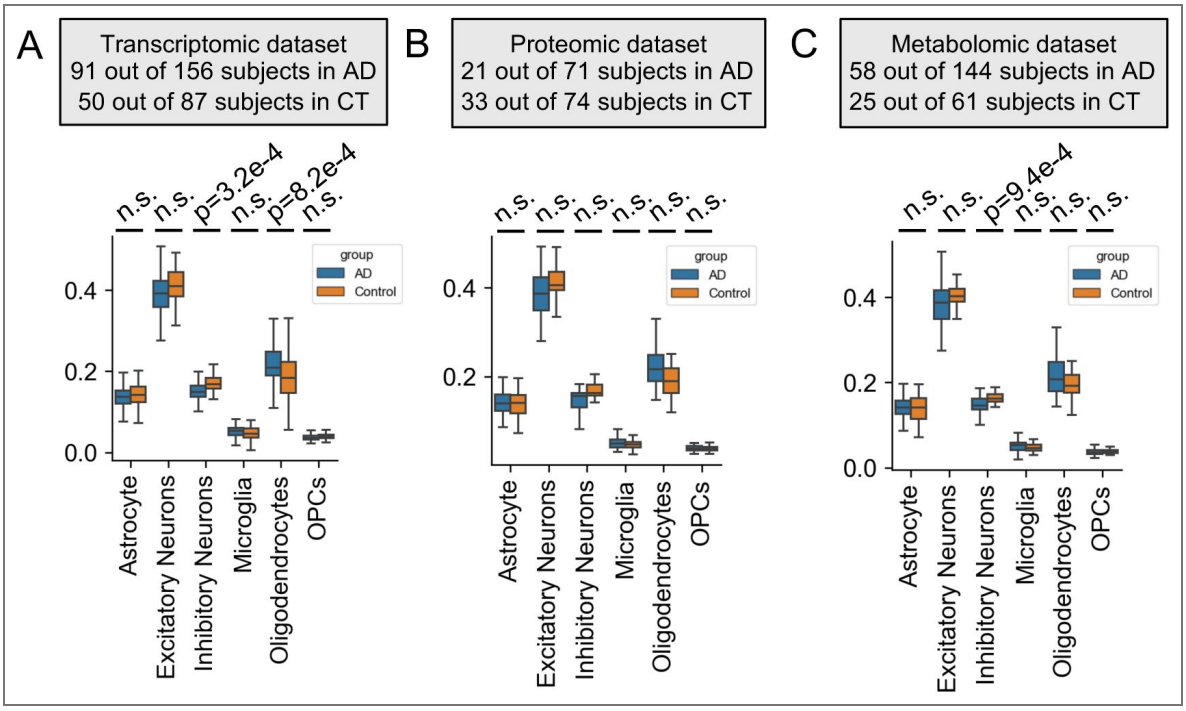

Figure S3. Cell type proportions estimation using a previous single-cell dataset.

Cell type proportions were estimated using a publicly available single-nucleus transcriptomic dataset from DLPFC tissue of 465 subjects in the ROSMAP cohort [84]. For each omic dataset, overlapping subjects were identified and cell type proportions were calculated for the matched samples. Box plots show the proportions of astrocytes, excitatory neurons, inhibitory neurons, microglia, oligodendrocytes, and OPCs in the AD group (blue) and the control group (orange) for the transcriptomic dataset (A; n = 91 AD, n = 50 CT), the proteomic dataset (B; n = 21 AD, n = 33 CT), and the metabolomic dataset (C; n = 58 AD, n = 25 CT). Statistical comparisons were performed using two-tailed t-tests with Bonferroni correction (significance threshold: p-value < 8.3×10^{-3}). n.s., not significant.

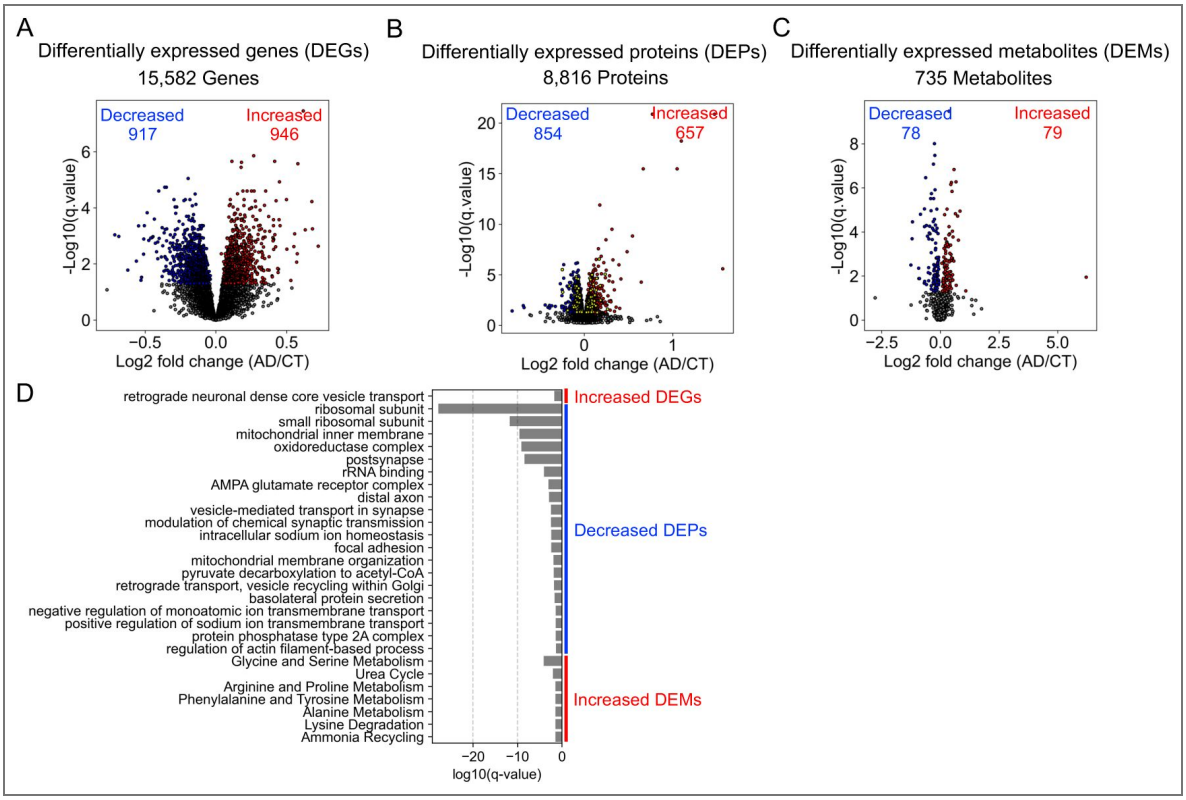

Figure S4. Differential and Enrichment analysis for differentially expressed molecules of AD.

(A) Volcano plot for differentially expressed genes in AD. Increased mRNAs are shown in red. Decreased mRNAs are shown in blue. (B) Volcano plot for differentially expressed proteins in AD. Increased proteins are shown in red. Decreased proteins are shown in blue. Differentially expressed enzyme proteins are shown in yellow. (C) Volcano plot for differentially expressed metabolites in AD. Increased metabolites are shown in red. Decreased metabolites are shown in blue. (D) Enrichment analysis for DEGs, DEPs, and DEMs in AD performed with Metascape (for DEGs and DEPs) and MetaboAnalyst (for DEMs). Only significantly enriched terms (q-value < 0.05) are shown.

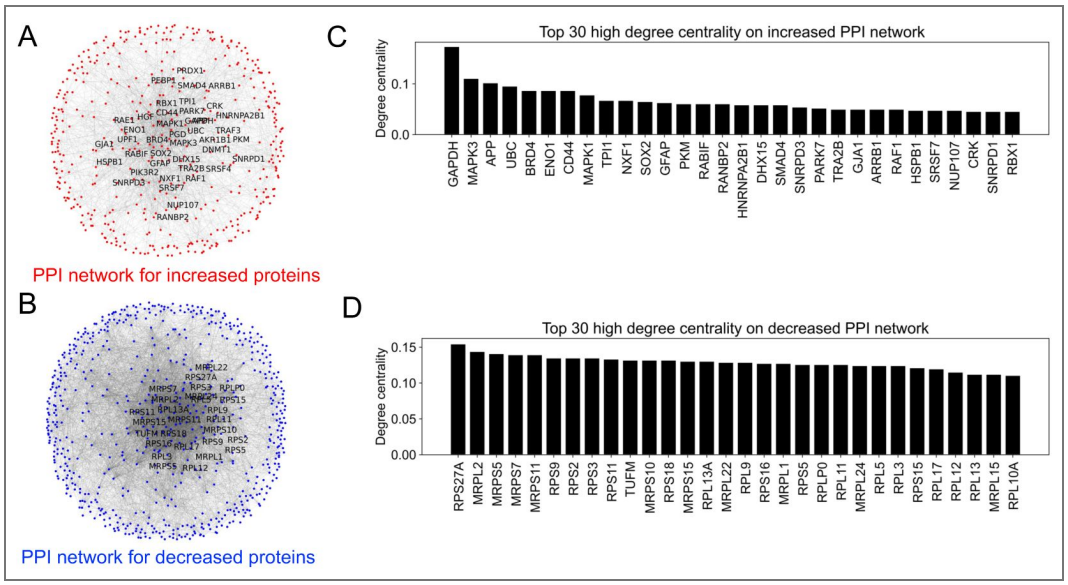

Figure S5. Construction of protein-protein interaction networks in DLPFC of AD.

(A) The protein-protein interaction (PPI) network for increased DEPs. Red nodes and gray edges indicated DEPs and their interactions, respectively. The nodes whose degree are over 18 their degree centralities are labeled for reasons of legibility (Supplementary Data 2). (B) The PPI network for decreased DEPs. Blue nodes and gray edges indicated DEPs and their interactions, respectively. The nodes whose degree are over 75 their degree centralities are labeled for reasons of legibility (Supplementary Data 2). (C) Top 30 DEPs with high degree centrality on the increased PPI network. (D) Top 30 DEPs with high degree centrality on the decreased PPI network.

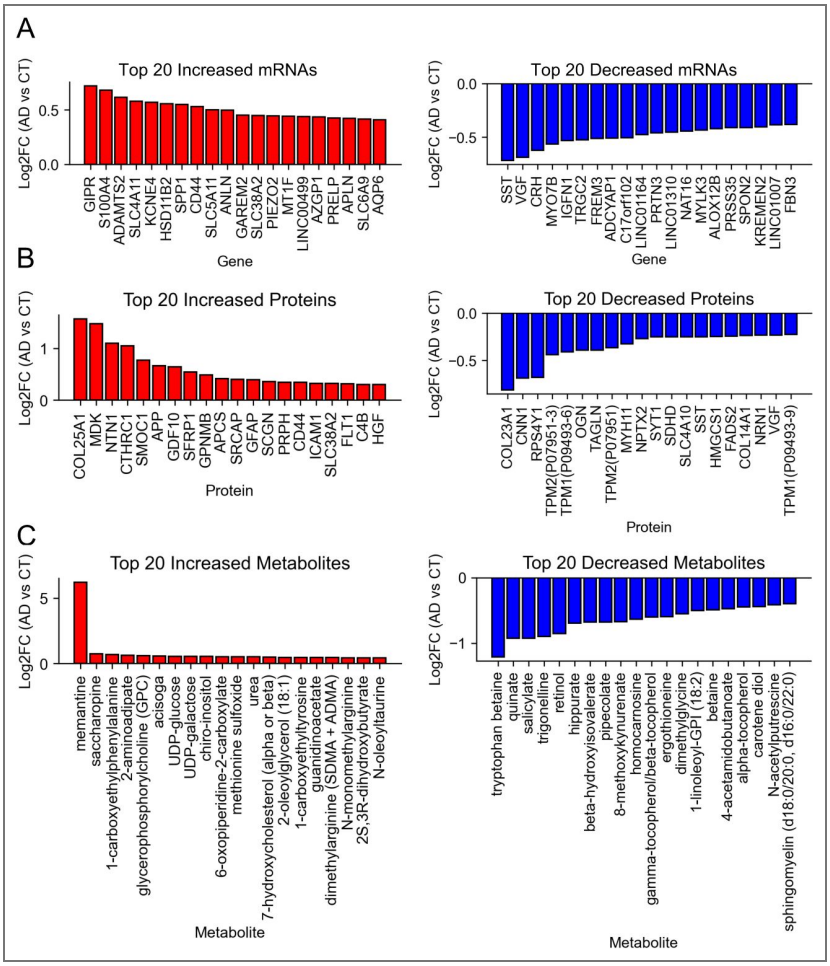

Figure S6. Top 20 differentially expressed genes, proteins, and metabolites.

(A) The top 20 differentially expressed genes (DEGs) ranked and plotted according to $\log_2$ fold change (Log2FC) in mean expression between AD and CT. Red, DEGs with increased expression in AD (left); blue, DEGs with decreased expression in AD (right). (B) The top 20 differentially expressed proteins (DEPs) ranked and plotted according to $\log_2$ fold change (Log2FC) in mean expression between AD and CT. Red, DEPs with increased expression in AD (left); blue, DEPs with decreased expression in AD (right). (C) The top 20 differentially expressed metabolites (DEMs) ranked and plotted according to $\log_2$ fold change (Log2FC) in mean expression between AD and CT. Red, DEMs with increased expression in AD (left); blue, DEMs with decreased expression in AD (right).

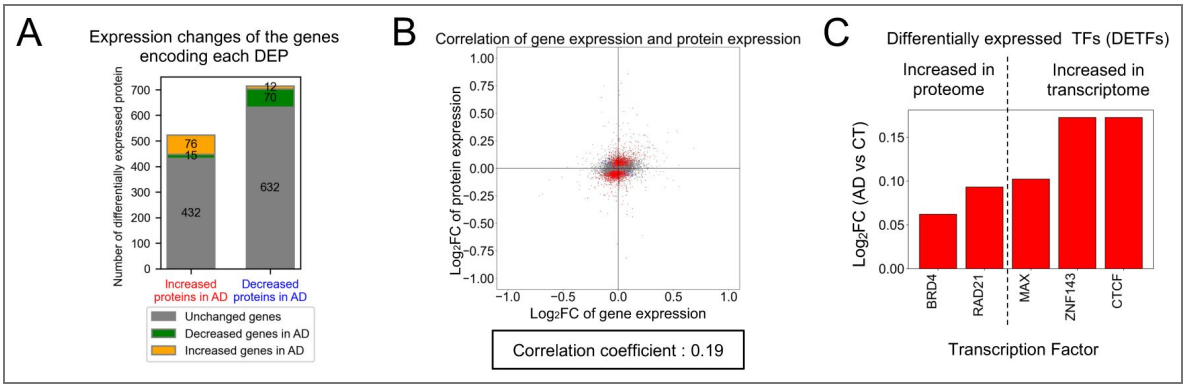

Figure S7. Identification of differential regulations connecting differentially expressed molecules across different omic layers.

(A) The change in the encoding gene for the corresponding DEP grouped according to the increased DEPs and decreased DEPs in AD. (B) Correlation of the $\log_2$ fold changes (AD group vs. CT group) of measured molecules at the transcriptome level (x-axis) and proteome level (y-axis). Each point on a scatter plot represents a molecule measured as both mRNA and protein. DEPs are shown in blue or red. Blue represents those DEPs with encoding DEGs that change in the opposite direction; Red represents the rest of the DEPs. (C) Log_2 fold change (AD group vs. CT group) of each differentially expressed transcription factor (DETF). The log2 fold change (Log2FC) of gene expression (transcriptome) or protein expression (proteome) of the indicated DETFs, which were identified from the 19 TFs that were inferred as potential regulators of DEGs with significantly altered expression in AD.

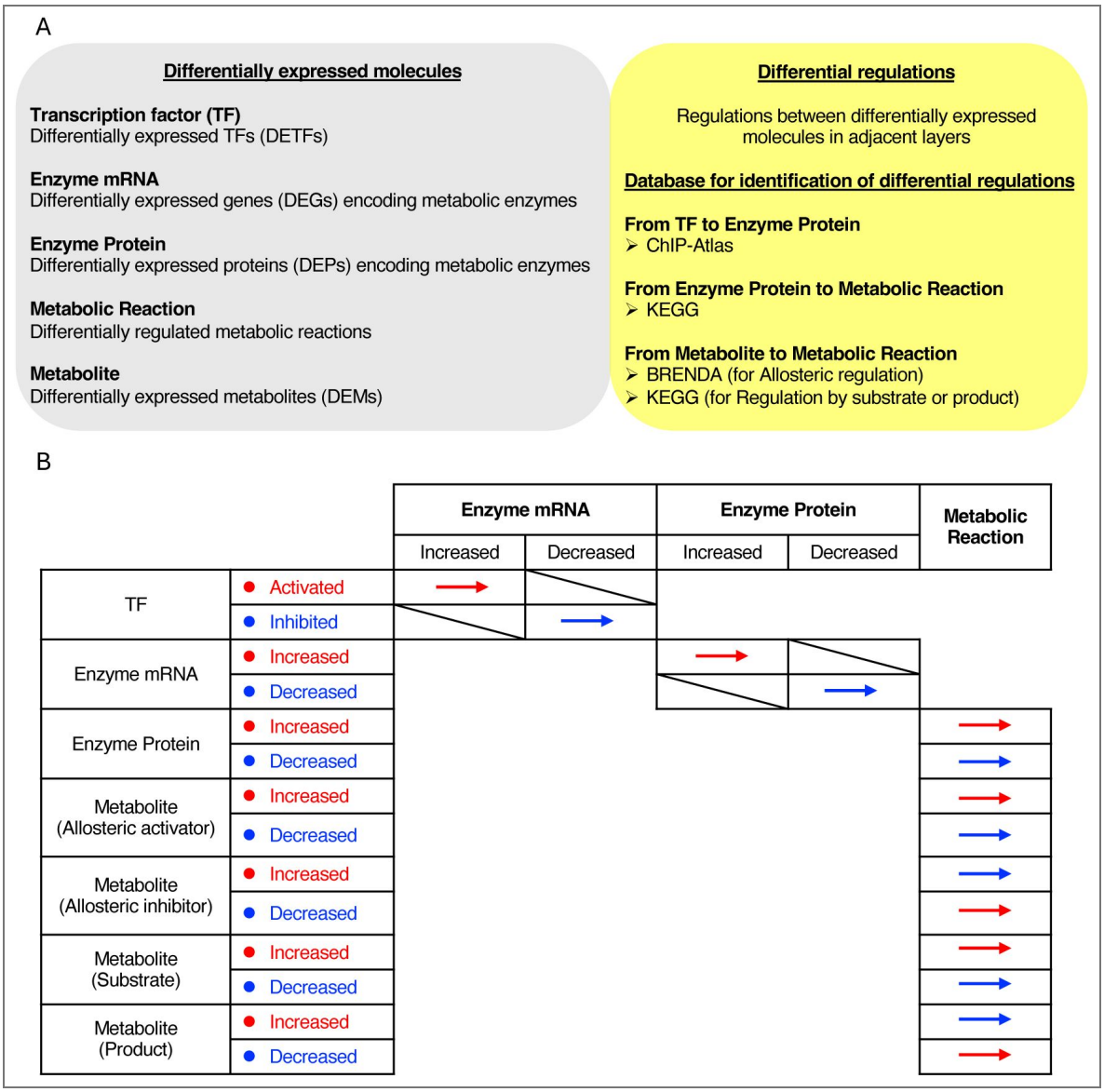

Figure S8. Contents of the trans-omic network for differentially regulated metabolic reactions between CT and AD.

(A) The definition of differentially expressed molecules in each layer (left). Differential regulations between adjacent layers and the databases used to identify them (right). (B) Classification of the differential regulations (activating or inhibiting in AD group). The methodology of constructing differential regulatory trans-omic network of metabolic reactions is based on our previous study [74,75]. Briefly, differentially expressed TFs (DETFs), genes (enzyme mRNAs), proteins (metabolic enzymes), metabolic reactions, and metabolites were integrated to construct a five-layer network for AD. Adjacent layers were linked by known regulatory relationships. Edge colors indicate the direction and functional sign of changes: red/blue denote activating/inhibiting regulation for TF-mRNA, mRNA-protein, and protein-reaction edges. For reaction-metabolite links, edge colors were assigned based on the metabolite change and its role (allosteric activator/inhibitor or substrate/product).

Supplementary text

Top 20 differentially expressed genes, proteins, metabolites. (Fig. S6)

We identified the top 20 increased and top 20 decreased DEGs based on their $\log_2$ fold change (log2FC) values (AD group vs. CT group) for their mean values (Fig. S6A).

GIPR, which has been reported to have neuroprotective effects [76], and the inflammation-associated gene *CD44* were identified as DEGs with high log2FC values. *SST*, encoding the neuropeptide somatostatin, was identified among the DEGs with the lowest log2FC values.

We also identified the top 20 upregulated and top 20 downregulated DEPs based on their $\log_2$ fold change (log2FC) values (Fig. S6B). DEPs with high log2FC values included SIRPB1, which promotes phagocytosis by microglia [77], and GFAP, a candidate blood biomarker of AD [78]. DEPs with low log2FC values included those associated with the cytoskeleton, such as CNN1, TMP1, and TMP2.

We also identified the top 20 DEMs with the highest and lowest log2 fold change (log2FC) values (Fig. S6C). Notably, memantine was identified as the metabolite with the highest log2FC value. Memantine is a therapeutic drug for Alzheimer's disease.

Therefore, it does not seem to be related to the pathology of the disease itself. However, this means that our analysis can accurately detect the differences between CT and AD groups. Retinol and sphingomyelin showed the lowest log2FC values.

Protein-protein interaction networks for the DEPs in AD. (Fig. S5)

The multi-omic data used in this study contains not only metabolism, but also more general cellular mechanisms such as gene-regulatory network and protein-protein interactions. Therefore, we constructed protein-protein interaction (PPI) networks using DEPs with STRING [79] (Fig. S5A, S5B and Supplementary Data 2). We then examined the degree centralities of the nodes on the PPI networks (Fig. S5C and S5D). In the "Increased PPI" network, GAPDH emerged as the protein with the highest degree centrality. GAPDH is not only an enzyme in the glycolytic pathway but also plays roles in apoptosis, neurodegeneration, cognitive dysfunction, and the formation of aggregates with Aβ [10]. In contrast, in the "Decreased PPI" network, nearly all the top 30 proteins by degree centrality were ribosomal proteins or mitochondrial ribosomal proteins. These results suggested that AD is associated with reduced translation both in nucleus and mitochondria.

Supplementary tables

Classification	TF Name
for Increased Gene	CTCF, MAX, MYCN, OLIG2, KDM1A, CTCFL, ARID1A, LIN28B, GTF3C2, CHD8, SMC3, ZNF92, TOP2B, ZNF143, EP300, TEAD4, BRD4, RAD21, BRD2
for Decreased Gene	None

Table S1. A list of transcription factors inferred to be involved in the regulation of DEGs in DLPFC of AD.

Increased enzymes	ACAT2, AK1, AKR1B1, ALDH3A2, AMPD2, ASL, B4GALNT1, BBOX1, BLVRA, BLVRB, CA3, CAD, CBR3, CBS, CMBL, DGKG, DNMT1, ENO1, ESD, FAH, GALK1, GALM, GALNT16, GAPDH, GBE1, GMPR, GSTP1, INPP4B, ITPKB, LPIN1, LTA4H, MAN2A2, MAOB, MTAP, MTHFD1, MTHFD2L, NAGK, NT5C, NUDT16, OCRL, PAFAH1B3, PGAM2, PGD, PGLS, PHYKPL, PI4K2A, PKM, PLCD1, PLCD3, PPT1, PRDX6, QPRT, RBKS, RENBP, SAT2, SORD, TPI1, UGP2, UROD
Decreased enzymes	ABHD16A, ACAA2, ACOX1, ACSS1, ADCY1, ADCY2, AGPAT1, AGPAT3, AHCYL1, ALDH4A1, ALPL, AOC3, BCAT2, BCKDHB, BDH1, BPNT2, CDIPT, CS, CTH, DBT, DGKH, DGKI, DGKZ, DLD, ECHS1, FADS2, FDFT1, GAD1, GAD2, GGT5, GK, GLDC, GPHN, GSTK1, HMGCL, HMGCS1, HMOX2, HSD17B12, IDH2, L2HGDH, LCLAT1, MBOAT2, MECR, MGLL, MGST3, MT-ND3, MTMR7, NAT8L, NDUFS1, NDUFS7, NDUFS8, NDUFV1, NFS1, NNT, NOS1, NT5E, PDE4A, PDE4B, PGM2L1, PIP5K1A, PIP5K1C, PLCB1, PRPS2, PYCR2, RRM1, SDHA, SETD7, SHMT2, SMPD3, TM7SF2

Table S2. A list of differentially expressed metabolic enzymes in DLPFC of AD.

Data availability

All raw omics data used for this study are available through the AD Knowledge Portal (*https://adknowledgeportal.org*). The AD Knowledge Portal is a platform for accessing data, analyses, and tools generated by the Accelerating Medicines Partnership (AMP-AD) Target Discovery Program and other National Institute on Aging (NIA)-supported programs to enable open-science practices and accelerate translational learning. The data, analyses and tools are shared early in the research cycle without a publication embargo on secondary use. Data are available for general research use according to the following requirements for data access and data attribution (*https://adknowledgeportal.synapse.org/Data%20Access*).

Acknowledgements

We thank Takashi Iwatsubo (The University of Tokyo), Kenichiro Sato (The University of Tokyo), Tadafumi Kato (Juntendo University), Katsuyuki Yugi (RIKEN), Junichi Maruyama (RIKEN), Kentaro Tomii (AIST), and Hafumi Nishi (Tohoku University), Tatsuhiko Tsunoda (The University of Tokyo) for valuable suggestions and discussions. We also thank our laboratory members for critically reading this manuscript.

This study was supported by the Japan Society for the Promotion of Science (JSPS) KAKENHI (JP21H04759), CREST, the Japan Science and Technology Agency (JST) (JPMJCR2123), JST ASPIRE (JPMJAP24B1), and by The Uehara Memorial Foundation. K.M. receives funding from a Grant-in-Aid for Early-Career Scientists (JP21K15342). H.W. was supported by AMED Grant Number JP21wm0425016.

The results published here are in whole or in part based on data obtained from the AD Knowledge Portal (*https://adknowledgeportal.org/*).

For the transcriptome data, we used the results of differential expression analysis based on RNA-seq measurements from ROSMAP participants as part of the RNA-seq Harmonization Study (*https://www.synapse.org/Synapse:syn8456721*). We utilized proteome data obtained from participants of the ROSMAP Study (*https://www.synapse.org/Synapse:syn21266454*). We used metabolome data acquired from ROSMAP Study participants (*https://www.synapse.org/Synapse:syn25985690*).

For validation of transcriptome data, we used the results of a differential expression analysis conducted using the same method on RNA-seq data from The Mount Sinai Brain Bank (MSBB) Study within the same research (*https://www.synapse.org/Synapse:syn10526259*). For validation of proteome data, we used the TMT-MS results from The Accelerating Medicines Partnership Alzheimer's Disease Diverse Cohorts Study (AMP-AD_DiverseCohorts) (*https://www.synapse.org/Synapse:syn55249985*). For cell type proportion analysis, we used snRNA-seq data from ROSMAP study participants (*https://www.synapse.org/Synapse:syn31512863*).

We used ChatGPT and DeepL for the assistance of manuscript editing and coding.

The authors thank Nancy R. Gough (BioSerendipity, LLC) for editorial assistance and critical input.

Additional information

Code availability

We utilized and modified the algorithm that was developed in our previous study, iTraNet (Sugimoto et al., 2024). The code used for the analysis in this paper is available upon request.

Author contributions

T.K. and S.K. conceived and supervised the project; T.K. and H.S. analyzed the data; writing group consisted of T.K., K.M., H.S., H.W., and S.K.

Funding

Funder	Grant reference number	Author
Grant-in-Aid for Early-Career Scientists	JP21K15342	Keigo Morita
Japan Agency for Medical Research and Development (AMED)	JP21wm0425016	Hirohisa Watanabe
Japan Society for the Promotion of Science KAKENHI	JP21H04759	Shinya Kuroda
CREST		Shinya Kuroda
Japan Science and Technology Agency (JST)	https://doi.org/10.52926/jpmjcr2123	Shinya Kuroda
Uehara Memorial Foundation (UMF)		Shinya Kuroda

Author ORCID iDs

Shinya Kuroda: https://orcid.org/0000-0001-5059-8299

Additional files

Supplementary Data 1 Trans-Omic network for metabolic reactions in AD.

Supplementary Data 2 Protein-protein interaction networks in AD.

References

1. **An Y,** Varma VR, Varma S, Casanova R, Dammer E, Pletnikova O, Chia CW, Egan JM, Ferrucci L, Troncoso J, *et al.* (2018) Evidence for brain glucose dysregulation in Alzheimer's disease. *Alzheimer's & Dementia: The Journal of the Alzheimer's Association* **14**:318-329 https://doi.org/10.1016/j.jalz.2017.09.011 | PubMed
2. **Arnold SE,** Arvanitakis Z, Macauley-Rambach SL, Koenig AM, Wang H.-Y, Ahima RS, Craft S, Gandy S, Buettner C, Stoeckel LE, *et al.* (2018) Brain insulin resistance in type 2 diabetes and Alzheimer disease: concepts and conundrums. *Nature Reviews. Neurology* **14**:168-181 https://doi.org/10.1038/nrneurol.2017.185 | PubMed
3. **Baloni P,** Funk CC, Yan J, Yurkovich JT, Kueider-Paisley A, Nho K, Heinken A, Jia W, Mahmoudiandehkordi S, Louie G, *et al.* (2020) Metabolic Network Analysis Reveals Altered Bile Acid Synthesis and Metabolism in Alzheimer's Disease. *Cell Reports Medicine* **1**:100138 https://doi.org/10.1016/j.xcrm.2020.100138 | PubMed
4. **Batra R,** Arnold M, Wörheide MA, Allen M, Wang X, Blach C, Levey AI, Seyfried NT, Ertekin-Taner N, Bennett DA, *et al.* (2023) The landscape of metabolic brain alterations in Alzheimer's disease. *Alzheimer's & Dementia: The Journal of the Alzheimer's Association* **19**:980-998 https://doi.org/10.1002/alz.12714 | PubMed
5. **Batra R,** Krumsiek J, Wang X, Allen M, Blach C, Kastenmüller G, Arnold M, Ertekin-Taner N, Kaddurah-Daouk R, Alzheimer's Disease Metabolomics Consortium (ADMC) (2024) Comparative brain metabolomics reveals shared and distinct metabolic alterations in Alzheimer's disease and progressive supranuclear palsy. *Alzheimer's & Dementia: The Journal of the Alzheimer's Association* **20**:8294-8307 https://doi.org/10.1002/alz.14249 | PubMed
6. **Beckmann ND,** Lin W.-J, Wang M, Cohain AT, Charney AW, Wang P, Ma W, Wang Y.-C, Jiang C, Audrain M, *et al.* (2020) Multiscale causal networks identify VGF as a key regulator of Alzheimer's disease. *Nature Communications* **11**:3942 https://doi.org/10.1038/s41467-020-17405-z | PubMed
7. **Bennett DA,** Buchman AS, Boyle PA, Barnes LL, Wilson RS, Schneider JA (2018) Religious Orders Study and Rush Memory and Aging Project. *Journal of Alzheimer's Disease: JAD* **64**:S161-S189 https://doi.org/10.3233/JAD-179939 | PubMed

8. **Bennett DA,** Schneider JA, Arvanitakis Z, Wilson RS (2012) Overview and findings from the religious orders study. *Current Alzheimer Research* **9**:628-645 https://doi.org/10.2174/156720512801322573 | PubMed

9. **Bonvento G,** Bolaños JP (2021) Astrocyte-neuron metabolic cooperation shapes brain activity. *Cell Metabolism* **33**:1546-1564 https://doi.org/10.1016/j.cmet.2021.07.006 | PubMed

10. **Breijyeh Z,** Karaman R (2020) Comprehensive Review on Alzheimer's Disease: Causes and Treatment. *Molecules* **25** https://doi.org/10.3390/molecules25245789 | PubMed

11. **Bubber P,** Haroutunian V, Fisch G, Blass JP, Gibson GE (2005) Mitochondrial abnormalities in Alzheimer brain: mechanistic implications. *Annals of Neurology* **57**:695-703 https://doi.org/10.1002/ana.20474 | PubMed

12. **Cahill KM,** Huo Z, Tseng GC, Logan RW, Seney ML (2018) Improved identification of concordant and discordant gene expression signatures using an updated rank-rank hypergeometric overlap approach. *Scientific Reports* **8**:9588 https://doi.org/10.1038/s41598-018-27903-2 | PubMed

13. **Chang A,** Jeske L, Ulbrich S, Hofmann J, Koblitz J, Schomburg I, Neumann-Schaal M, Jahn D, Schomburg D (2021) BRENDA, the ELIXIR core data resource in 2021: new developments and updates. *Nucleic Acids Research* **49**:D498-D508 https://doi.org/10.1093/nar/gkaa1025 | PubMed

14. **De Jager PL,** Ma Y, McCabe C, Xu J, Vardarajan BN, Felsky D, Klein H.-U, White CC, Peters MA, Lodgson B, *et al.* (2018) A multi-omic atlas of the human frontal cortex for aging and Alzheimer's disease research. *Scientific Data* **5**:180142 https://doi.org/10.1038/sdata.2018.142 | PubMed

15. **de la Monte SM,** Tong M (2014) Brain metabolic dysfunction at the core of Alzheimer's disease. *Biochemical Pharmacology* **88**:548-559 https://doi.org/10.1016/j.bcp.2013.12.012 | PubMed

16. **Egami R,** Kokaji T, Hatano A, Yugi K, Eto M, Morita K, Ohno S, Fujii M, Hironaka K.-I, Uematsu S, *et al.* (2021) Trans-omic analysis reveals obesity-associated dysregulation of inter-organ metabolic cycles between the liver and skeletal muscle. *iScience* **24**:102217 https://doi.org/10.1016/j.isci.2021.102217 | PubMed

17. **Fu W,** Shi D, Westaway D, Jhamandas JH (2015) Bioenergetic mechanisms in astrocytes may contribute to amyloid plaque deposition and toxicity. *The Journal of Biological Chemistry* **290**:12504-12513 https://doi.org/10.1074/jbc.M114.618157 | PubMed

18. **Green GS,** Fujita M, Yang H.-S, Taga M, Cain A, McCabe C, Comandante-Lou N, White CC, Schmidtner AK, Zeng L, *et al.* (2024) Cellular communities reveal trajectories of brain ageing and Alzheimer's disease. *Nature* **633**:634-645 https://doi.org/10.1038/s41586-024-07871-6 | PubMed

19. **Hannon E,** Dempster EL, Davies JP, Chioza B, Blake GET, Burrage J, Policicchio S, Franklin A, Walker EM, Bamford RA, *et al.* (2024) Quantifying the proportion of different cell types in the human cortex using DNA methylation profiles. *BMC Biology* **22**:17 https://doi.org/10.1186/s12915-024-01827-y | PubMed

20. **Hansmannel F,** Sillaire A, Kamboh MI, Lendon C, Pasquier F, Hannequin D, Laumet G, Mounier A, Ayral A.-M, DeKosky ST, *et al.* (2010) Is the urea cycle involved in Alzheimer's disease?. *Journal of Alzheimer's Disease: JAD* **21**:1013-1021 https://doi.org/10.3233/JAD-2010-100630 | PubMed

21. **Hernández-Ortega K,** Garcia-Esparcia P, Gil L, Lucas JJ, Ferrer I (2016) Altered machinery of protein synthesis in Alzheimer's: From the nucleolus to the ribosome. *Brain Pathology* **26**:593-605 https://doi.org/10.1111/bpa.12335 | PubMed

22. **Horgusluoglu E,** Neff R, Song W.-M, Wang M, Wang Q, Arnold M, Krumsiek J, Galindo-Prieto B, Ming C, Nho K, *et al.* (2022) Integrative metabolomics-genomics approach reveals key metabolic pathways and regulators of Alzheimer's disease. *Alzheimer's & Dementia: The Journal of the Alzheimer's Association* **18**:1260-1278 https://doi.org/10.1002/alz.12468 | PubMed

23. **Jankowska-Kulawy A,** Klimaszewska-Łata J, Gul-Hinc S, Ronowska A, Szutowicz A (2022) Metabolic and cellular compartments of acetyl-CoA in the healthy and diseased brain. *International Journal of Molecular Sciences* **23**:10073 https://doi.org/10.3390/ijms231710073 | PubMed

24. **Jensen NJ,** Wodschow HZ, Nilsson M, Rungby J (2020) Effects of Ketone Bodies on Brain Metabolism and Function in Neurodegenerative Diseases. *International Journal of Molecular Sciences* **21** https://doi.org/10.3390/ijms21228767 | PubMed

25. **Jia D,** Wang F, Yu H (2023) Systemic alterations of tricarboxylic acid cycle enzymes in Alzheimer's disease. *Frontiers in Neuroscience* **17**:1206688 https://doi.org/10.3389/fnins.2023.1206688 | PubMed

26. **Johnson ECB,** Carter EK, Dammer EB, Duong DM, Gerasimov ES, Liu Y, Liu J, Betarbet R, Ping L, Yin L, *et al.* (2022) Large-scale deep multi-layer analysis of Alzheimer's disease brain reveals strong proteomic disease-related changes not observed at the RNA level. *Nature Neuroscience* **25**:213-225 https://doi.org/10.1038/s41593-021-00999-y | PubMed

27. **Johnson ECB,** Dammer EB, Duong DM, Ping L, Zhou M, Yin L, Higginbotham LA, Guajardo A, White B, Troncoso JC, *et al.* (2020) Large-scale proteomic analysis of Alzheimer's disease brain and cerebrospinal fluid reveals early changes in energy metabolism associated with microglia and astrocyte activation. *Nature Medicine* **26**:769-780 https://doi.org/10.1038/s41591-020-0815-6 | PubMed

28. **Ju YH,** Bhalla M, Hyeon SJ, Oh JE, Yoo S, Chae U, Kwon J, Koh W, Lim J, Park YM, *et al.* (2022) Astrocytic urea cycle detoxifies Aβ-derived ammonia while impairing memory in Alzheimer's disease. *Cell Metabolism* **34**:1104-1120.e8. https://doi.org/10.1016/j.cmet.2022.05.011 | PubMed

29. **Kanehisa M,** Furumichi M, Sato Y, Matsuura Y, Ishiguro-Watanabe M (2025) KEGG: biological systems database as a model of the real world. *Nucleic Acids Research* **53**:D672-D677 https://doi.org/10.1093/nar/gkae909 | PubMed

30. **Koepsell H** (2020) Glucose transporters in brain in health and disease. *Pflugers Archiv: European Journal of Physiology* **472**:1299-1343 https://doi.org/10.1007/s00424-020-02441-x | PubMed

31. **Kokaji T,** Eto M, Hatano A, Yugi K, Morita K, Ohno S, Fujii M, Hironaka K.-I, Ito Y, Egami R, *et al.* (2022) In vivo transomic analyses of glucose-responsive metabolism in skeletal muscle reveal core differences between the healthy and obese states. *Scientific Reports* **12**:13719 https://doi.org/10.1038/s41598-022-17964-9 | PubMed

32. **Koschützki D,** Schreiber F (2008) Centrality analysis methods for biological networks and their application to gene regulatory networks. *Gene Regulation and Systems Biology* **2**:193-201 https://doi.org/10.4137/grsb.s702 | PubMed

33. **Kumar V,** Kim S.-H, Bishayee K (2022) Dysfunctional Glucose Metabolism in Alzheimer's Disease Onset and Potential Pharmacological Interventions. *International Journal of Molecular Sciences* **23** https://doi.org/10.3390/ijms23179540 | PubMed

34. **Kyrtata N,** Emsley HCA, Sparasci O, Parkes LM, Dickie BR (2021) A Systematic Review of Glucose Transport Alterations in Alzheimer's Disease. *Frontiers in Neuroscience* **15**:626636 https://doi.org/10.3389/fnins.2021.626636 | PubMed

35. **Leventhal MJ,** Zanella CA, Kang B, Peng J, Gritsch D, Liao Z, Bukhari H, Wang T, Pao P.-C, Danquah S, *et al.* (2024) An integrative systems-biology approach defines mechanisms of Alzheimer's disease neurodegeneration. *bioRxiv* https://doi.org/10.1101/2024.03.17.585262 | PubMed

36. **Liang WS,** Reiman EM, Valla J, Dunckley T, Beach TG, Grover A, Niedzielko TL, Schneider LE, Mastroeni D, Caselli R, *et al.* (2008) Alzheimer's disease is associated with reduced expression of energy metabolism genes in posterior cingulate neurons. *Proceedings of the National Academy of Sciences of the United States of America* **105**:4441-4446 https://doi.org/10.1073/pnas.0709259105 | PubMed

37. **Liu Y,** Liu F, Iqbal K, Grundke-Iqbal I, Gong C.-X (2008) Decreased glucose transporters correlate to abnormal hyperphosphorylation of tau in Alzheimer disease. *FEBS Letters* **582**:359-364 https://doi.org/10.1016/j.febslet.2007.12.035 | PubMed

38. **Maffioli E,** Murtas G, Rabattoni V, Badone B, Tripodi F, Iannuzzi F, Licastro D, Nonnis S, Rinaldi AM, Motta Z, *et al.* (2022) Insulin and serine metabolism as sex-specific hallmarks of Alzheimer's disease in the human hippocampus. *Cell Reports* **40**:111271 https://doi.org/10.1016/j.celrep.2022.111271 | PubMed

39. **Magistretti PJ,** Allaman I (2015) A cellular perspective on brain energy metabolism and functional imaging. *Neuron* **86**:883-901 https://doi.org/10.1016/j.neuron.2015.03.035 | PubMed

40. **Martin FJ,** Amode MR, Aneja A, Austine-Orimoloye O, Azov AG, Barnes I, Becker A, Bennett R, Berry A, Bhai J, *et al.* (2023) Ensembl 2023. *Nucleic Acids Research* **51**:D933-D941 https://doi.org/10.1093/nar/gkac958 | PubMed

41. **Mathys H,** Boix CA, Akay LA, Xia Z, Davila-Velderrain J, Ng AP, Jiang X, Abdelhady G, Galani K, Mantero J, *et al.* (2024) Single-cell multiregion dissection of Alzheimer's disease. *Nature* **632**:858-868 https://doi.org/10.1038/s41586-024-07606-7 | PubMed

42. **Matuszewska M,** Cieślik M, Wilkaniec A, Strawski M, Czapski GA (2022) The role of bromodomain and extraterminal (BET) proteins in controlling the phagocytic activity of microglia in vitro: Relevance to Alzheimer's disease. *International Journal of Molecular Sciences* **24**:13 https://doi.org/10.3390/ijms24010013 | PubMed

43. **Moon S,** Lee H (2022) MOMA: a multi-task attention learning algorithm for multi-omics data interpretation and classification. *Bioinformatics* **38**:2287-2296 https://doi.org/10.1093/bioinformatics/btac080 | PubMed

44. **Mosconi L,** Mistur R, Switalski R, Tsui WH, Glodzik L, Li Y, Pirraglia E, De Santi S, Reisberg B, Wisniewski T, *et al.* (2009) FDG-PET changes in brain glucose metabolism from normal cognition to pathologically verified Alzheimer's disease. *European Journal of Nuclear Medicine and Molecular Imaging* **36**:811-822 https://doi.org/10.1007/s00259-008-1039-z | PubMed

45. **Nikkar R,** Esmaeili-Bandboni A, Badrikoohi M, Babaei P (2022) Effects of inhibiting astrocytes and BET/BRD4 chromatin reader on spatial memory and synaptic proteins in rats with Alzheimer's disease. *Metabolic Brain Disease* **37**:1119-1131 https://doi.org/10.1007/s11011-022-00940-7 | PubMed

46. **Novotny BC,** Fernandez MV, Wang C, Budde JP, Bergmann K, Eteleeb AM, Bradley J, Webster C, Ebl C, Norton J, *et al.* (2023) Metabolomic and lipidomic signatures in autosomal dominant and late-onset Alzheimer's disease brains. *Alzheimer's & Dementia: The Journal of the Alzheimer's Association* **19**:1785-1799 https://doi.org/10.1002/alz.12800 | PubMed

47. **Paglia G,** Stocchero M, Cacciatore S, Lai S, Angel P, Alam MT, Keller M, Ralser M, Astarita G (2016) Unbiased Metabolomic Investigation of Alzheimer's Disease Brain Points to Dysregulation of Mitochondrial Aspartate Metabolism. *Journal of Proteome Research* **15**:608-618 https://doi.org/10.1021/acs.jproteome.5b01020 | PubMed

48. **Pang Z,** Lu Y, Zhou G, Hui F, Xu L, Viau C, Spigelman AF, MacDonald PE, Wishart DS, Li S, *et al.* (2024) MetaboAnalyst 6.0: towards a unified platform for metabolomics data processing, analysis and interpretation. *Nucleic Acids Research* **52**:W398-W406 https://doi.org/10.1093/nar/gkae253 | PubMed

49. **Parker WD,** Parks J, Filley CM, Kleinschmidt-DeMasters BK (1994) Electron transport chain defects in Alzheimer's disease brain. *Neurology* **44**:1090-1096 https://doi.org/10.1212/wnl.44.6.1090 | PubMed

50. **Plaisier SB,** Taschereau R, Wong JA, Graeber TG (2010) Rank-rank hypergeometric overlap: identification of statistically significant overlap between gene-expression signatures. *Nucleic Acids Research* **38**:e169 https://doi.org/10.1093/nar/gkq636 | PubMed

51. **Reddy JS,** Heath L, Linden AV, Allen M, Lopes K. de P, Seifar F, Wang E, Ma Y, Poehlman WL, Quicksall ZS, *et al.* (2024) Bridging the gap: Multi-omics profiling of brain tissue in Alzheimer's disease and older controls in multi-ethnic populations. *Alzheimer's & Dementia: The Journal of the Alzheimer's Association* **20**:7174-7192 https://doi.org/10.1002/alz.14208 | PubMed

52. **Scheltens P,** De Strooper B, Kivipelto M, Holstege H, Chételat G, Teunissen CE, Cummings J, van der Flier WM (2021) Alzheimer's disease. *The Lancet* **397**:1577-1590 https://doi.org/10.1016/S0140-6736(20)32205-4 | PubMed

53. **Shireby G,** Dempster EL, Policicchio S, Smith RG, Pishva E, Chioza B, Davies JP, Burrage J, Lunnon K, Seiler Vellame D, *et al.* (2022) DNA methylation signatures of Alzheimer's disease neuropathology in the cortex are primarily driven by variation in non-neuronal cell-types. *Nature Communications* **13**:5620

https://doi.org/10.1038/s41467-022-33394-7 | PubMed

54. **Simpson IA,** Chundu KR, Davies-Hill T, Honer WG, Davies P (1994) Decreased concentrations of GLUT1 and GLUT3 glucose transporters in the brains of patients with Alzheimer's disease. *Annals of Neurology* **35**:546-551 https://doi.org/10.1002/ana.410350507 | PubMed

55. **Steen E,** Terry BM, Rivera EJ, Cannon JL, Neely TR, Tavares R, Xu XJ, Wands JR, de la Monte SM (2005) Impaired insulin and insulin-like growth factor expression and signaling mechanisms in Alzheimer's disease--is this type 3 diabetes?. *Journal of Alzheimer's Disease: JAD* **7**:63-80 https://doi.org/10.3233/jad-2005-7107 | PubMed

56. **Sugimoto H,** Morita K, Li D, Bai Y, Mattanovich M, Kuroda S (2024) iTraNet: a web-based platform for integrated trans-omics network visualization and analysis. *Bioinformatics Advances* **4**:vbae141 https://doi.org/10.1093/bioadv/vbae141 | PubMed

57. **Sun J,** Gui Y, Zhou S, Zheng X.-L (2024) Unlocking the secrets of aging: Epigenetic reader BRD4 as the target to combatting aging-related diseases. *Journal of Advanced Research* **63**:207-218 https://doi.org/10.1016/j.jare.2023.11.006 | PubMed

58. **Swerdlow RH** (2020) The mitochondrial hypothesis: Dysfunction, bioenergetic defects, and the metabolic link to Alzheimer's disease. *International Review of Neurobiology* **154**:207-233 https://doi.org/10.1016/bs.irn.2020.01.008 | PubMed

59. **Szablewski L** (2021) Brain Glucose Transporters: Role in Pathogenesis and Potential Targets for the Treatment of Alzheimer's Disease. *International Journal of Molecular Sciences* **22** https://doi.org/10.3390/ijms22158142 | PubMed

60. **Szklarczyk D,** Kirsch R, Koutrouli M, Nastou K, Mehryary F, Hachilif R, Gable AL, Fang T, Doncheva NT, Pyysalo S, *et al.* (2023) The STRING database in 2023: protein-protein association networks and functional enrichment analyses for any sequenced genome of interest. *Nucleic Acids Research* **51**:D638-D646 https://doi.org/10.1093/nar/gkac1000 | PubMed

61. **Tasaki S,** Xu J, Avey DR, Johnson L, Petyuk VA, Dawe RJ, Bennett DA, Wang Y, Gaiteri C (2022) Inferring protein expression changes from mRNA in Alzheimer's dementia using deep neural networks. *Nature Communications* **13**:655 https://doi.org/10.1038/s41467-022-28280-1 | PubMed

62. **Varma VR,** Wang Y, An Y, Varma S, Bilgel M, Doshi J, Legido-Quigley C, Delgado JC, Oommen AM, Roberts JA, *et al.* (2021) Bile acid synthesis, modulation, and dementia: A metabolomic, transcriptomic, and pharmacoepidemiologic study. *PLoS Medicine* **18**:e1003615 https://doi.org/10.1371/journal.pmed.1003615 | PubMed

63. **Wan Y.-W,** Al-Ouran R, Mangleburg CG, Perumal TM, Lee TV, Allison K, Swarup V, Funk CC, Gaiteri C, Allen M, *et al.* (2020) Meta-Analysis of the Alzheimer's Disease Human Brain Transcriptome and Functional Dissection in Mouse Models. *Cell Reports* **32**:107908 https://doi.org/10.1016/j.celrep.2020.107908 | PubMed

64. **Wang J,** Liao N, Du X, Chen Q, Wei B (2024) A semi-supervised approach for the integration of multi-omics data based on transformer multi-head self-attention mechanism and graph convolutional networks. *BMC Genomics* **25**:86 https://doi.org/10.1186/s12864-024-09985-7 | PubMed

65. **Wang M,** Li A, Sekiya M, Beckmann ND, Quan X, Schrode N, Fernando MB, Yu A, Zhu L, Cao J, *et al.* (2021) Transformative network modeling of multi-omics data reveals detailed circuits, key regulators, and potential therapeutics for Alzheimer's Disease. *Neuron* **109**:257-272.e14. https://doi.org/10.1016/j.neuron.2020.11.002 | PubMed

66. **Xu J,** Begley P, Church SJ, Patassini S, Hollywood KA, Jüllig M, Curtis MA, Waldvogel HJ, Faull RLM, Unwin RD, *et al.* (2016) Graded perturbations of metabolism in multiple regions of human brain in Alzheimer's disease: Snapshot of a pervasive metabolic disorder. *Biochimica et Biophysica Acta* **1862**:1084-1092 https://doi.org/10.1016/j.bbadis.2016.03.001 | PubMed

67. **Yan X,** Hu Y, Wang B, Wang S, Zhang X (2020) Metabolic Dysregulation Contributes to the Progression of Alzheimer's Disease. *Frontiers in Neuroscience* **14**:530219 https://doi.org/10.3389/fnins.2020.530219 | PubMed

68. **Yu L,** Jin J, Xu Y, Zhu X (2022) Aberrant Energy Metabolism in Alzheimer's Disease. *Journal of Translational Internal Medicine* **10**:197-206 https://doi.org/10.2478/jtim-2022-0024 | PubMed

69. **Zhou Y,** Zhou B, Pache L, Chang M, Khodabakhshi AH, Tanaseichuk O, Benner C, Chanda SK (2019) Metascape provides a biologist-oriented resource for the analysis of systems-level datasets. *Nature Communications* **10**:1523 https://doi.org/10.1038/s41467-019-09234-6 | PubMed

70. **Zou Z,** Ohta T, Oki S (2024) ChIP-Atlas 3.0: a data-mining suite to explore chromosome architecture together with large-scale regulome data. *Nucleic Acids Research* **52**:W45-W53 https://doi.org/10.1093/nar/gkae358 | PubMed

71. **Paglia G,** Stocchero M, Cacciatore S, et al. (2016) Unbiased Metabolomic Investigation of Alzheimer's Disease Brain Points to Dysregulation of Mitochondrial Aspartate Metabolism. *J Proteome Res* **15**:608-618 https://doi.org/10.1021/acs.jproteome.5b01020 | PubMed

72. **Xu J,** Begley P, Church SJ, et al. (2016) Graded perturbations of metabolism in multiple regions of human brain in Alzheimer's disease: Snapshot of a pervasive metabolic disorder. *Biochim Biophys Acta* **1862**:1084-1092 https://doi.org/10.1016/j.bbadis.2016.03.001 | PubMed

73. **Maffioli E,** Murtas G, Rabattoni V, et al. (2022) Insulin and serine metabolism as sex-specific hallmarks of Alzheimer's disease in the human hippocampus. *Cell Rep* **40**:111271 https://doi.org/10.1016/j.celrep.2022.111271 | PubMed

74. **Bai Y,** Morita K, Kokaji T, Hatano A, Ohno S, Egami R, Pan Y, Li D, Yugi K, Uematsu S, *et al.* (2024) Trans-omic analysis reveals opposite metabolic dysregulation between feeding and fasting in liver associated with obesity. *iScience* **27**:109121 https://doi.org/10.1016/j.isci.2024.109121 | PubMed

75. **Egami R,** Kokaji T, Hatano A, Yugi K, Eto M, Morita K, Ohno S, Fujii M, Hironaka KI, Uematsu S, *et al.* (2021) Trans-omic analysis reveals obesity-associated dysregulation of inter-organ metabolic cycles between the liver and skeletal muscle. *iScience* **24**:102217 https://doi.org/10.1016/j.isci.2021.102217 | PubMed

76. **Reich N,** Hölscher C (2022) The neuroprotective effects of glucagon-like peptide 1 in Alzheimer's and Parkinson's disease: An in-depth review. *Frontiers in neuroscience* **16**:970925 https://doi.org/10.3389/fnins.2022.970925 | PubMed

77. **Gaikwad S,** Larionov S, Wang Y, et al. (2009) Signal regulatory protein-beta1: a microglial modulator of phagocytosis in Alzheimer's disease. *Am J Pathol* **175**:2528-2539 https://doi.org/10.2353/ajpath.2009.090147 | PubMed

78. **Kim KY,** Shin KY, Chang KA (2023) GFAP as a Potential Biomarker for Alzheimer's Disease: A Systematic Review and Meta-Analysis. *Cells* **12**:1309 https://doi.org/10.3390/cells12091309 | PubMed

79. **Szklarczyk D,** Kirsch R, Koutrouli M, et al. (2023) The STRING database in 2023: protein-protein association networks and functional enrichment analyses for any sequenced genome of interest. *Nucleic Acids Res* **51**:D638-D646 https://doi.org/10.1093/nar/gkac1000 | PubMed

80. **Lazarev VF,** Tsolaki M, Mikhaylova ER, Benken KA, Shevtsov MA, Nikotina AD, Lechpammer M, Mitkevich VA, Makarov AA, Moskalev AA, *et al.* (2021) Extracellular GAPDH Promotes Alzheimer Disease Progression by Enhancing Amyloid-β Aggregation and Cytotoxicity. *Aging and disease* **12**:1223-1237 https://doi.org/10.14336/AD.2020.1230 | PubMed

81. **Wan Y.-W,** Al-Ouran R, Mangleburg CG, Perumal TM, Lee TV, Allison K, Swarup V, Funk CC, Gaiteri C, Allen M, *et al.* (2020) Meta-Analysis of the Alzheimer's Disease Human Brain Transcriptome and Functional Dissection in Mouse Models. *Cell Reports* **32**:107908 https://doi.org/10.1016/j.celrep.2020.107908 | PubMed

82. **Batra R,** Krumsiek J, Wang X, Allen M, Blach C, Kastenmüller G, Arnold M, Ertekin-Taner N, Kaddurah-Daouk R, Alzheimer's Disease Metabolomics Consortium (ADMC) (2024) Comparative brain metabolomics reveals shared and distinct metabolic alterations in Alzheimer's disease and progressive supranuclear palsy. *Alzheimer's & Dementia: The Journal of the Alzheimer's Association* **20**:8294-8307 https://doi.org/10.1002/alz.14249 | PubMed

83. **Novotny BC,** Fernandez MV, Wang C, Budde JP, Bergmann K, Eteleeb AM, Bradley J, Webster C, Ebl C, Norton J, *et al.* (2023) Metabolomic and lipidomic signatures in autosomal dominant and late-onset Alzheimer's disease brains. *Alzheimer's & Dementia: The Journal of the Alzheimer's Association* **19**:1785-1799 https://doi.org/10.1002/alz.12800 | PubMed

84. **Green GS,** Fujita M, Yang H.-S, Taga M, Cain A, McCabe C, Comandante-Lou N, White CC, Schmidtner AK, Zeng L, *et al.* (2024) Cellular communities reveal trajectories of brain ageing and Alzheimer's disease. *Nature* **633**:634-645 https://doi.org/10.1038/s41586-024-07871-6 | PubMed

Wan YW, Al-Ouran R, Mangleburg CG, et al (2020) Differential Expression Results. Synapse. ID syn8456721 https://www.synapse.org/Synapse:syn8456721

Johnson ECB, Dammer EB, Duong DM, et al (2020) C2.median_polish_corrected_log2(abundanceRatioCenteredOnMedianOfBatchMediansPerProtein)-8817x400. Synapse. ID syn21266454 https://www.synapse.org/Synapse:syn21266454

Batra R, Arnold M, Wörheide MA, et al (2023) ROSMAP_Metabolon_HD4_Brain514_assay_data. Synapse. ID syn25985690 https://www.synapse.org/Synapse:syn25985690

Wan YW, Al-Ouran R, Mangleburg CG, et al (2020) Differential Expression Results (Tissue.Diagnosis). Synapse. ID syn10526259 https://www.synapse.org/Synapse:syn10526259

Reddy JS, Heath L, Linden AV, et al (2024) n1086_residual_log2_batch. Synapse. ID syn55249985 https://www.synapse.org/Synapse:syn55249985

Green GS, Fujita M, Yang HS, et al (2024) Gene Expression (snRNAseq - DLPFC, Experiment 2). Synapse. ID syn31512863 https://www.synapse.org/Synapse:syn31512863

Peer reviews

Reviewer #1 (Public review):

The authors aim to reconstruct a multi-layer metabolic regulatory network in Alzheimer's disease by integrating transcriptomic, proteomic, and metabolomic datasets from human brain tissue. By linking transcription factors, enzyme expression, metabolic reactions, and metabolites, the study seeks to provide a systems-level understanding of disease-associated metabolic dysregulation.

The revised manuscript has improved in clarity and includes additional analyses in response to prior comments, particularly the incorporation of cell-type proportion estimates derived from matched single-cell datasets. This represents a meaningful step toward addressing concerns about the interpretation of bulk tissue and strengthens the study's descriptive rigor.

However, several key limitations remain. First, although cell-type proportions are now estimated, this information is not integrated into downstream analyses. As a result, it remains unclear whether the observed metabolic changes reflect cell-intrinsic regulation or shifts in cellular composition. This distinction is critical for interpreting the inferred regulatory network and limits the strength of the conclusions.

Second, the biological conclusions remain largely confirmatory. The reported downregulation of energy-related pathways, including the TCA cycle and oxidative phosphorylation, is consistent with prior literature. The trans-omic framework provides a structured representation of these changes, but the manuscript does not convincingly demonstrate that this approach yields new mechanistic insight beyond existing knowledge. In particular, the network is not sufficiently leveraged to identify novel regulatory relationships or generate testable hypotheses.

Third, while the framework integrates multiple molecular layers, the contribution of upstream transcriptional regulation remains unclear. The most compelling findings appear to arise from protein and metabolite layers, and the manuscript does not clearly demonstrate

how transcription factors or mRNA-level changes contribute to the interpretation of metabolic dysregulation. This weakens the claim that the study provides a fully integrated trans-omic perspective.

Fourth, concerns regarding network robustness remain. The analysis relies on partially overlapping cohorts across omics modalities, and although this limitation is acknowledged, no formal sensitivity or robustness analyses are presented. This reduces confidence in the stability and generalizability of the inferred network structure.

Finally, the handling of covariates remains limited. While the authors justify this based on data availability and prior studies, the lack of consistent adjustment for known confounders introduces uncertainty in attributing observed differences specifically to disease-related biology.

Overall, the study presents a technically sound application of a trans-omic integration framework and provides a coherent overview of metabolic dysregulation in Alzheimer's disease. However, the findings are primarily descriptive and confirmatory, and the current analyses do not fully demonstrate that the approach yields novel biological insight. The work will be of interest to researchers in systems biology and multi-omics integration, but its impact on advancing understanding of disease mechanisms is likely to be moderate.

https://doi.org/10.7554/eLife.111228.1.sa1

Author response:

General Statements:

We appreciate the reviewers for the critical review of the manuscript and the valuable comments. We have carefully considered the reviewer's comments and have revised our manuscript accordingly.

Point-by-point description of the revisions:

> ***Reviewer #1 (Evidence, reproducibility and clarity):***
>
> *Major comments*
>
> *(1) This study leaves out lipid metabolism as a major energy metabolism pathway relevant to AD. The authors themselves cite the significance of acylcarnitines and CPT1A in AD (pg. 3, lines 32-33, pg. 4, lines 1-2). Lipid metabolism and homeostasis is known to be disrupted in AD1. Fatty acid oxidation is a known energy source in the prefrontal cortex2 and will also generate acetyl coA, which this study reveals is a significant decreased metabolite in AD. Furthermore, sphingomyelin emerges as one of the major decreased DEMs as well. Thus, lipid metabolism should be highlighted in Figure 3 and discussed throughout the manuscript; otherwise its omission should be clearly stated and justified.*

We appreciate the reviewer's insightful comment regarding a critical role of lipid metabolism in AD. We recognize that lipid metabolism is a metabolic pathway deeply involved in AD pathology (Baloni et al., 2022, 2020; Varma et al., 2021). Accordingly, we have revised the **Limitations** section to more strongly emphasize its role as a vital energy source (pg. 13, lines 15-17). Regarding the visualization of lipid metabolism, we extracted lipid-related pathway from the trans-omic network but found that the regulatory relationships among DEPs and DEMs were excessively complex and interconnected. Thus, interpreting this regulatory network seemed to be more challenging compared to the other energy production pathways presented in our manuscript. Therefore, we have concluded that the pathway analysis in our trans-omic network may not be suitable for deeply elucidating the lipid dysregulation in AD.

We have added a statement acknowledging this as a limitation of our current methodology in the revised manuscript (pg. 13, lines 13-22).

> *(2) The covariates used for differential analysis should be discussed and justified. Notably, age is used as a covariate for transcriptomic analysis but not proteomic and metabolomic analysis, with no justification. Additionally, given the known importance of lipid metabolism in AD and the putative role of APOE in lipid homeostasis3, APOE genetic status should be considered as a covariate, or its omission should be justified.*

We appreciate the reviewer's comment regarding the included covariates in differential analyses of our study. The reason we did not include other variables, such as age at death and RIN, is that these data were not available for each sample. Thus, we referred to the original research articles from which proteomic or metabolomic datasets used in our study were derived. Regarding the metabolomic dataset, in the original article (Batra et al., 2023), only two metabolites, 1-methyl-5-imidazoleacetate and N6-carboxymethyllysine, were significantly associated with age. In addition, no metabolites were significantly associated with sex, BMI, and years of education. Regarding the proteomic dataset, in the original article (Johnson et al., 2020), age at death, PMI, and sex were included as covariates in the analyses, though these variables were not found to strongly influence the data (Extended Data Fig.2 in (Johnson et al., 2020)).

> *(3) The authors make a conclusion statement that suggests intervention: "Collectively, our data suggests that preserving or improving the ability to produce ATP and early intervention in the process of nitrogen metabolism are candidates for the prevention and treatment of dementia" (pg. 12, lines 12-14). This claim is not well-supported by the evidence provided in the study. There are a few limitations: (a) This was an observational, not interventional study; (b) The study did not establish whether the metabolic disruptions are causes or effects in AD; and (c) ATP or other bioenergetic indicators were not directly measured. Therefore, any statements about potential interventions should be removed or qualified as highly speculative.*

We agree with the reviewer that the statement regarding potential interventions was not sufficiently supported by our analyses. Accordingly, we have removed the sentence regarding prevention and treatment from the revised manuscript (e.g., we have deleted final paragraph of the previous manuscript).

> *(4) In conjunction with the last point, the main conclusion of the study is that energy production is down in AD. The data presented in Figure 3 are consistent with this conclusion, but it is far from definitive due to limitations stated above in comments 3a and 3b. The authors should offer additional support for this conclusion: experimental follow-up, flux modeling, analysis of alternative datasets with ATP measurement, causal inference.*

We sincerely thank the reviewer for this valuable and constructive suggestion. Regarding flux modeling, we agree that metabolic flux analysis could provide important mechanistic insight. Indeed, previous studies have applied flux modeling in the context of lipid metabolism in Alzheimer's disease (Baloni et al., 2022). We also attempted to perform flux modeling focusing on energy metabolism. However, we found it difficult to obtain biologically meaningful and robust results and therefore decided not to include these analyses in the current manuscript.

With respect to ATP measurements, we fully agree that direct evidence of altered ATP levels would further strengthen our conclusion. However, to the best of our knowledge, there are currently no publicly available large-scale datasets that directly measure ATP levels in human postmortem brain tissues. This limitation makes it challenging to incorporate validation in the present study.

Regarding experimental follow-up, we agree that functional validation is essential to confirm the mechanistic implications of our findings. We are actively considering follow-up experimental studies. However, we consider the present work to be a multi-omic integrative analysis aimed at identifying key molecular alterations and generating biologically important hypotheses. We have revised the Limitation section to more clearly position this manuscript as an observational systems-level analysis (pg. 13, lines 20-22).

> *(5) The validation analysis did not sufficiently show the generalizability of this study's results. The authors demonstrated a correlation of 0.53 to the MSBB transcriptomics data and 0.60 to the AMP-AD DiverseCohorts proteomics data. Beyond these correlation coefficients, no meaningful comparison between the datasets is offered. How concordant are the differentially expressed features (or pathways) between the datasets? How robust would the trans-omic network be if incorporating the alternate datasets? Is the main conclusion (energy metabolism is down in AD) supported by the validation datasets? We think this analysis should be expanded and described in the main text.*
>
> *Although the results for external metabolomics datasets are reported in Fig S2C, correlation coefficients with the external data are not reported. The authors state, "Note that each study used different definitions for AD and CT groups, had variations in measurement methods and brain regions analyzed." We appreciate these limitations. However, the external data should be re-analyzed using the same definitions of AD and CT, if possible. The limitations and results (which DEMs are shared between datasets) should be discussed in the main text.*

We thank the reviewer for this important comment regarding the generalizability of our findings. In the revised manuscript, we have expanded the validation analyses and summarized the results in Figure S2. First, at the transcriptomic level, Figure S2B and S2C show the overlap between up- and downregulated genes in AD identified in our ROSMAP-derived analyses and those reported in a previously published large-scale meta-analysis of 2,114 postmortem samples across seven brain regions (Wan et al., 2020). A substantial proportion of DEGs were shared, supporting cross-cohort and cross-region robustness to some extent. At the proteomic level, Figure S2E shows a comparison between the ROSMAP and the AMP-AD DiverseCohorts datasets. We highlighted the subset of enzymes involved in the energy metabolism analysis shown in Fig. 3 and calculated a separate correlation coefficient for this subset (Pearson coefficient = 0.86, p-value = 1.5e-7), further supporting our main conclusion. In addition, to assess the concordance between the two datasets in a threshold-independent manner, we additionally performed Rank-Rank Hypergeometric Overlap (RRHO) analysis (Figure S2E). RRHO analysis (Cahill et al., 2018; Plaisier et al., 2010) enables the comparison of ranked protein lists without relying on arbitrary differential expression cutoffs and has been used for cross-dataset comparison in several previous studies (Fröhlich et al., 2024; Maitra et al., 2023). The RRHO heatmaps demonstrated significant enrichment in the concordant quadrants, confirming systematic agreement between datasets beyond simple correlation coefficients. For metabolomics, Figure S2G shows RRHO analyses comparing the ROSMAP metabolomic data with other datasets measured by the same UPLC-MS/MS platform (Batra et al., 2024; Novotny et al., 2023), demonstrating significant concordance in ranked metabolite changes in AD.

> *(6) The glycolysis analysis and discussion needs more development. Glycolysis and gluconeogenesis share many of the same enzymes, but they are not the same pathway and should not be discussed as such. To make a claim about the overall influence of enzyme and metabolite levels on glycolysis, the authors should focus on the energetically committing steps of glycolysis (hexokinase, phosphofructokinase, pyruvate kinase) in Figure 3A, and include the full/current version of the figure in the supplement. Gluconeogenesis-specific enzymes (pyruvate carboxylase, PEPCK) are not mentioned at all - are they among the DEPs/DEGs?*

We appreciate the reviewer's comment regarding the distinction between glycolysis and gluconeogenesis pathway. Among the gluconeogenesis-specific enzyme proteins, G6PC1, FBP1, PC, and PCK2 were measured in our dataset, but none of them were identified as DEPs. In addition, gluconeogenesis is a process that occurs primarily in the liver and kidney rather than the brain. Given this biological context and the lack of significant changes in relevant enzymes, we have revised the terminology throughout the manuscript, replacing "glycolysis/gluconeogenesis pathway" with "glycolysis pathway" in the revised version.

> *(7) Given that there wasn't good concordance between the DEGs and DEPs, did including the mRNA and transcription factor layers in the network really add anything useful? It seems like the main conclusions of the manuscript were driven by the protein and metabolite layers only. How many of the DE metabolic enzymes were coregulated at the transcript and protein level? It would be useful to include the 5-layer trans-omic network in the supplement to display these results. Given your network, at what level does it appear that energy metabolism is regulated?*

It is true that our primary conclusion regarding the regulation of energy metabolism is driven by the changes in protein and metabolite abundance. However, we consider the low concordance between mRNA and protein expression itself to be an important feature of AD pathology, as also reported in previous studies (Johnson et al., 2022; Tasaki et al., 2022). Although we did not perform a further analysis of this discordance, we believe that including the TF and mRNA layers into the metabolic trans-omic network strengthens a system-wide view of metabolic dysregulation in AD.

Regarding the mRNA changes corresponding to the DEP enzymes, please refer to Figure S7A.

> *(8) Comment further on the results from Figure 2D. What can be learned from identifying metabolites with the greatest degree centrality? What pathways other than energy metabolism are highlighted by the trans-omic network?*

We assume that some energetic indicators, including AMP and acetyl-CoA, and nitrogen metabolism-related metabolites, Glu, 2-oxoglutarate, and urea, can be potential key regulators of dysregulated metabolism in AD.

> *(9) (Suggestion) We suggest the authors leverage their trans-omic network in additional ways beyond giving a snapshot of a few energy metabolism pathways. The analysis of top DEMs could go further. What pathways are impacted beyond energy metabolism? Among the metabolic reactions allosterically regulated by top DEMs, what metabolic pathways are enriched?*

We identified the enriched metabolic pathways that were allosterically regulated by DEMs in AD using Fisher's exact test. Alanine, aspartate, and glutamate metabolism pathways were significantly enriched in 2-oxoglutarate, glutarate, alanine, and glutamate-regulating metabolic reactions. Arginine and proline metabolism pathway was enriched in N-methyl-L-arginine and putrescine-regulating metabolic reactions. Arginine biosynthesis pathway was enriched in arginine-regulating metabolic reactions. Glycerophospholipid metabolism pathway was enriched in CDP-ethanolamine-regulating metabolic reactions. Glycine, serine,

and threonine metabolism pathway was enriched in serine-regulating metabolic reactions. Purine metabolism pathway was enriched in AMP-regulating metabolic reactions. Pyrimidine metabolism pathway was enriched in deoxyuridine and thymidine-regulating metabolic reactions. Sphingolipid metabolism pathway was enriched in sphingosine-regulating metabolic reactions. However, this analysis did not yield sufficiently valuable insights into the regulatory relationships among biomolecules in AD. Thus, we did not include these results in the revised manuscript.

> *(10) (Suggestion) Figure 3 shows that most differential signal in AD points to lower energy production due to the combination of differentially expressed metabolites and enzymes, but we are not given much context about the strength of these among all the differential signals. We would suggest including volcano plots where the features of interest, i.e. DE enzymes and metabolites, are colored differently (or a similar figure).*

We thank the reviewer for this constructive suggestion. To provide better context regarding the importance of the differential signals, we have added volcano plots for mRNAs, proteins, and metabolites in Figure S4A, B, and C.

> *(11) (Suggestion) The PPI network could be better leveraged to understand metabolic changes in AD. If nodes are grouped into subnetworks (e.g. by Louvain / Leiden clustering) and tested for pathway enrichment, could you find functional subnetworks of coordinately up- and down- regulated metabolic enzymes? This could yield some pathways of interest beyond the energy metabolism pathways already highlighted.*

We appreciate the reviewer's suggestion to utilize the PPI network for subnetwork analysis. However, it is important to note that the proteomic dataset analyzed in this study is derived from the original work of (Johnson et al., 2020). In that paper, the authors already performed a Weighted Gene Co-expression Network Analysis (WGCNA) across several datasets to identify co-expressed modules and functional pathways.

Given this, we assumed that applying additional clustering methods to the same dataset would be unlikely to yield significant biological insights beyond the established findings.

> *Minor comments*
>
> *(1). "All genes" and "all metabolites" should not be the background for the proteomic and metabolic pathway enrichment analysis by Metascape and MetaboAnalyst. The background should be limited to the proteins and metabolites that were measured.*

We fully agree with the reviewer that using "all gene" or "all metabolites" as a background is not suitable for enrichment analyses. As suggested, we have revised the enrichment analyses using the measured proteins and metabolites as a background in both Metascape and MetaboAnalyst (Fig. S4D).

> *(2) Highlight the metabolic enzymes in Fig S2B. Calculate a separate correlation coefficient for the enzymes extracted in the energy metabolism analysis from Fig 3.*

We appreciate the reviewer's suggestion to refine the correlation analysis. As requested, we have revised Fig. S2D to explicitly highlight the subset of enzymes involved in the energy metabolism analysis shown in Fig. 3. We calculated a separate correlation coefficient for the subset (Pearson coefficient = 0.86, p-value = 1.5e-7).

> *(3) Use a multiple hypothesis adjusted p-value or q-value in Figure S3.*

We agree with the reviewer regarding the necessity of correcting for multiple comparisons. Accordingly, we have revised Fig. S4D using q-values.

> *(4) Describe the methods used to calculate the logFC values from the validation dataset.*

We have revised the Methods to include a detailed description of the procedure used to calculate the log2FC values for the validation datasets (pg. 21, lines 13-15).

> *(5) It is difficult to read Figure 3. We would recommend really emphasizing to the reader to refer to Fig S7B as a "key" to this figure. The description of the red/blue arrows and nodes in the methods section (pg. 24, lines 21-36, pg 25, lines 1-4) were also helpful, but very lengthy. We recommend putting an abridged version of this description into the Fig S7 figure legend.*

We appreciate the feedback regarding the readability of Fig. 3. As recommended, we have revised the manuscript to explicitly direct readers to Fig. S8B as an essential “key” for interpreting the network visualization (pg. 8, lines 28). Furthermore, we have added an abridged description of the network elements to the legend of Fig. S8B.

> *(6) The S7 figure legend should refer to panels A and B, not E and F.*

We apologize for this oversight. We have corrected the legend of Fig. S8.

> *(7) (Suggestion) Are any of the differentially expressed metabolites allosteric regulators of the DE transcription factors? This could be interesting to discuss.*

We appreciate the reviewer’s insightful suggestion about the potential allosteric regulation of the DETFs by DEMs. We conducted an extensive literature search to identify any reports related to this perspective. However, to the best of our knowledge, no such direct interactions have been reported to date.

> ***Reviewer #1 (Significance):***
>
> *The study's strength lies in leveraging three omics modalities across large patient cohorts (n ~ 150-240) to identify coherent signals between transcriptomics, proteomics, and metabolomics in postmortem DLPFC tissue. It was encouraging to see that the main result, showing downregulation for TCA, oxidative phosphorylation, and ketone body metabolism, emerged from consistent signals across both proteomics and metabolomics. This result was consistent with previous findings in other models cited by the author4,5 and other studies 6,7 demonstrating deficiency in energy-producing pathways in AD.*
>
> *Another strength of the study is the application of thoughtful methodology to connect differentially expressed proteins and metabolites via an intermediate data layer of metabolic reactions. The authors leverage the KEGG and BRENDA databases and apply sound logic to estimate the effects of enzyme level and metabolite level on pathway activity, with metabolites serving as substrate, product, or allosteric regulator for reactions. This trans-omic network methodology was developed in previous studies cited by the author8,9.*
>
> *However, as written, this study is limited in its contribution of new knowledge to the AD research field. The main conclusion (energy production is down in AD, due to regulatory disruption of energy metabolism) is not strongly supported (see comments 1, 3, and 4 for elaboration). The evidence could be improved by orthogonal approaches: further experimentation, further integration of external datasets, causal modeling, or flux modeling. Alternatively, even in the absence of new experimental and computational approaches, the story could be made more complete by further leveraging the trans-omic network to provide insights into (a) the regulation of energy metabolism; and (b) the impacts of key disrupted metabolites (see comments 7-9).*
>
> *The study is also limited in its demonstrating the power of these methodologies to provide integrative insights. As mentioned above, the integration of enzyme levels and*

> *metabolite levels is clearly useful (Figure 3). In contrast, the utility of the mRNA and transcription factor layers was not evident. The study did not appear to improve or expand upon trans-omic network methodology described in the previous works. Finally, the various analyses (analyzing the trans-omic network for nodes with the highest degree centrality, the PPI analysis, and viewing the energy metabolism pathways in the network) provided disparate results that were only tenuously connected in the discussion section.*
>
> ***Reviewer #2 (Evidence, reproducibility and clarity):***
>
> *Summary*
>
> *This manuscript integrates public transcriptomic, proteomic, and metabolomic datasets from ROSMAP DLPFC samples to construct a multi-layer metabolic trans-omic network in Alzheimer's disease. By linking transcription factors, enzyme mRNAs, proteins, metabolic reactions, and metabolites, the authors report coordinated downregulation of the TCA cycle, oxidative phosphorylation, and ketone body metabolism, along with mixed regulatory signals in glycolysis/gluconeogenesis. They interpret these patterns as indicative of broad energetic dysfunction and alterations in amino-acid/nitrogen metabolism in AD. While the framework is conceptually appealing, much of the analysis remains descriptive, and several biological interpretations extend beyond what the data can robustly support. The reliance on bulk tissue without accounting for cell-type composition, limited covariate adjustment, and the absence of validation or sensitivity analyses reduce confidence in the mechanistic conclusions. Overall, the study provides a preliminary systems-level overview, but additional rigor is needed before the proposed trans-omic regulatory insights can be considered convincing.*
>
> *Major Comments*
>
> *(1) Interpretation requires more cautious phrasing, and validation is essential. The manuscript frequently asserts that specific pathways are "inhibited" or that energetic deficits are "compensated," but these conclusions extend beyond what the descriptive, bulk-level data can support. Because no metabolic flux, causality, or direct functional measurements are included, the results should be framed as putative regulatory shifts, not confirmed impairments. Critically, key claims about pathway inhibition would require flux modeling, perturbation analyses, or experimental validation to be convincing. Without such validation, the mechanistic interpretations remain speculative.*

We thank the reviewer for this crucial comment. We fully agree that, given the descriptive and bulk-level nature of our analysis, mechanistic interpretations must be made with caution. In the absence of direct metabolic flux measurements or experimental validation, our findings should be interpreted as putative regulatory shifts rather than confirmed functional impairments. Accordingly, we have revised the manuscript to temper mechanistic claims. We have replaced definitive statements with more speculative phrasing (e.g., “Our analysis revealed a putative coordinated downregulation …” instead of “Our analysis revealed a coordinated downregulation …” in Abstract section; “we demonstrate the systems-level view of the potential dysregulated energy production …” instead of “we demonstrate the systems-level view of the dysregulated energy production …” in pg. 10, lines 25-26).

> *(2) Although the authors acknowledge this in the limitations, bulk-level differences may primarily reflect altered proportions of neurons, astrocytes, microglia, and oligodendrocytes rather than true within-cell-type regulation. Incorporating a cell-type deconvolution or performing a sensitivity analysis would substantially improve interpretability. This issue also impacts the trans-omic network: if the molecules included originate from different cell types, the inferred regulatory relationships may not reflect true intracellular processes.*

We appreciate the reviewer's point that bulk-level differences can reflect altered proportions of different brain cell types, subsequently affecting the inferred trans-omic network analysis. To assess the changes in cell type proportions of the samples that we used in our study, we additionally used public single-cell transcriptomic datasets, which were obtained from DLPFC tissue of 465 subjects in the ROSMAP cohort (Green et al., 2024). For each omic data that we used in our analyses, we matched the same subjects and calculated the following cell type proportions, astrocytes, excitatory neurons, inhibitory neurons, microglias, oligodendrocytes, and OPCs. Then, we statistically compared the cell type proportions between control subjects and patients with AD (Fig. S3). In the transcriptomic data, we confirmed that the proportion of inhibitory neurons in the AD group was smaller than in the CT group, and that the proportion of oligodendrocytes in the AD group was larger than in the CT group. In the proteomic data, we did not observe any statistically significant changes in the cell type proportion between the two group. In the metabolomic data, we found that the proportion of inhibitory neurons in the AD group was smaller than in the CT group (pg. 6, lines 8-11).

> *(3) Differential analysis covariates. For the differential expression analyses, only gender and PMI were included as covariates. Additional variables, such as age at death, RIN, neuropathological measures, and comorbidities, can strongly influence molecular profiles and should be considered to ensure that the observed differences reflect AD-related biology rather than confounding pathological or technical factors.*

We appreciate the reviewer's comment regarding the included covariates in differential analyses of our study. The reason we did not include other variables, including age at death and RIN, is that these data for each sample were not available. Thus, we referred to original research articles from which proteomic or metabolomic datasets used in our study were derived. Regarding the metabolomic dataset, in the original article (Batra et al., 2023), only two metabolites, 1-methyl-5-imidazoleacetate and N6-carboxymethyllysine, were significantly associated with age. In addition, no metabolites were significantly associated with sex, BMI, or education. Regarding the proteomic dataset, in the original article, age at death, PMI, and sex were included as covariates in the analyses, though these variables were not found to strongly influence the data (Extended Data Fig.2 in (Johnson et al., 2020)).

> *(4) Network stability and sample non-overlap. Proteomic, transcriptomic, and metabolomic data come from partially overlapping individuals. The authors should test whether the reconstructed network is robust to: different significance thresholds, restricting analyses to overlapping samples and alternative definitions of AD vs control.*

We appreciate the reviewer's comment for the trans-omic network stability. In our study, the number of individuals for whom all omic modalities were measured was relatively small (n=25 in CT and n=35 in AD). This limited overlap reduces statistical power and can affect the downstream network construction. We have acknowledged this limitation in the revised manuscript and clarified that the reconstructed networks should be interpreted with caution regarding reproducibility and generalizability (pg. 13, lines 13-23).

> *Minor Comments*
>
> *(1) Some TF enrichment and regulatory inferences lack explicit mention of multiple-testing correction.*

We apologize for the lack of clarity in our original description. We have corrected for multiple-testing for the TF inference. Thus, we have revised the Methods section to explicitly describe the correction method used and the threshold applied (pg. 23, lines 23-24).

> *(2) The limitations section is strong but should explicitly discuss the influence of postmortem interval on metabolite levels.*

We appreciate the reviewer's comment about the effect of postmortem interval on changes in metabolite levels. Accordingly, we have added the description of this perspective in our revised manuscript (pg. 13, lines 1-5).

> ***Reviewer #2 (Significance):***
>
> *The study extends a trans-omic integration framework, originally applied to metabolic disease, into the context of Alzheimer's pathology. Although the biological findings largely confirm known alterations in mitochondrial and energy metabolism, the network-based approach offers a structured way to view cross-layer regulatory changes. Its main advance is conceptual rather than biological, providing a unified framework rather than uncovering fundamentally new mechanisms. This work will primarily interest researchers in neurodegeneration and systems biology, as well as computational groups developing multi-omics integration methods.*
>
> ***Reviewer #3 (Evidence, reproducibility and clarity):***
>
> *This study leverages existing transcriptomic, metabalomic and proteomic datasets from prefrontal cortex (PFC) to assess metabolic dysregulation in Alzheimer's disease (AD). They found a downregulation of multiple metabolic pathways, including TCA cycle, oxidative phosphorylation, and ketone metabolism, that may explain bioenergetic alterations in AD.*
>
> *The study used matching ROSMAP omics datasets from the DLPFC that have allowed more robust data integration. However, the datasets are all generated using bulk tissue, which makes data interpretation difficult. For example, the AD changes they observed may be due to shifts in cell type proportion with disease (e.g. cell death, neuron inflammation). Did the authors account for any potential shifts in cell type proportion in their analysis?*
>
> *If the assumption is that the changes in AD are cell intrinsic, which cell types are likely to be impacted? Can the authors integrate any existing single-cell analysis to infer which cell types may be driving the signals they detect, and whether this accounts for some of the antagonistic regulatory effects that were detected?*

We thank the reviewer for their insightful comments. We agree that the use of bulk tissue datasets cannot account for cell-type heterogeneity. As noted in our Limitations section (pg. 12, lines 24-27), we recognize that previous studies have found that the Braak stage is correlated positively with microglia and astrocyte proportions and negatively with oligodendrocyte proportion (Hannon et al., 2024; Shireby et al., 2022). Regarding the integration of single-cell analysis, we have referenced recent snRNA-seq findings (Mathys et al., 2024) in our Limitations section (pg. 12, lines 28-32) to deconvolve our bulk signatures.

Furthermore, in our revised manuscript, we additionally used public single-cell transcriptomic datasets, which were obtained from DLPFC tissue of 465 subjects in the ROSMAP cohort (Green et al., 2024). For each omic data that we used in our analyses, we matched the same subjects and calculated the following cell type proportions, astrocytes, excitatory neurons, inhibitory neurons, microglia, oligodendrocytes, and OPCs. Then, we statistically compared the cell type proportions between control subjects and patients with AD (Fig. S3). In the transcriptomic data, we confirmed that the proportion of inhibitory neurons in the AD group was smaller than in the CT group, and that the proportion of oligodendrocytes in the AD group was larger than in the CT group. In the proteomic data, we did not observe any statistically significant changes in the cell type proportion between the two groups. In the metabolomic data, we found that the proportion of inhibitory neurons in the AD group was smaller than in the CT group (pg. 6, lines 8-11).

> ***Reviewer #3 (Significance):***
>
> *The manuscript provides multimodal insight into metabolic dysregulation in AD in the PFC. Given that metabolic dysfunction is likely to play a major in disease pathogenesis, this is a study of importance. However, the findings lack granularity at the cell type level, which limits the impact of the study.*

Reference

(1) Baloni, P., Arnold, M., Buitrago, L., Nho, K., Moreno, H., Huynh, K., Brauner, B., Louie, G., Kueider-Paisley, A., Suhre, K., Saykin, A. J., Ekroos, K., Meikle, P. J., Hood, L., Price, N. D., Alzheimer's Disease Metabolomics Consortium, Doraiswamy, P. M., Funk, C. C., Hernández, A. I., … Kaddurah-Daouk, R. (2022). Multi-Omic analyses characterize the ceramide/sphingomyelin pathway as a therapeutic target in Alzheimer's disease. Communications Biology, 5(1), 1074.

(2) Baloni, P., Funk, C. C., Yan, J., Yurkovich, J. T., Kueider-Paisley, A., Nho, K., Heinken, A., Jia, W., Mahmoudiandehkordi, S., Louie, G., Saykin, A. J., Arnold, M., Kastenmüller, G., Griffiths, W. J., Thiele, I., Alzheimer's Disease Metabolomics Consortium, Kaddurah-Daouk, R., & Price, N. D. (2020). Metabolic Network Analysis Reveals Altered Bile Acid Synthesis and Metabolism in Alzheimer's Disease. Cell Reports. Medicine, 1(8), 100138.

(3) Batra, R., Arnold, M., Wörheide, M. A., Allen, M., Wang, X., Blach, C., Levey, A. I., Seyfried, N. T., Ertekin-Taner, N., Bennett, D. A., Kastenmüller, G., Kaddurah-Daouk, R. F., Krumsiek, J., & Alzheimer's Disease Metabolomics Consortium (ADMC). (2023). The landscape of metabolic brain alterations in Alzheimer's disease. Alzheimer's & Dementia: The Journal of the Alzheimer's Association, 19(3), 980–998.

(4) Batra, R., Krumsiek, J., Wang, X., Allen, M., Blach, C., Kastenmüller, G., Arnold, M., Ertekin-Taner, N., Kaddurah-Daouk, R., & Alzheimer's Disease Metabolomics Consortium (ADMC). (2024). Comparative brain metabolomics reveals shared and distinct metabolic alterations in Alzheimer's disease and progressive supranuclear palsy. Alzheimer's & Dementia: The Journal of the Alzheimer's Association, 20(12), 8294–8307.

(5) Cahill, K. M., Huo, Z., Tseng, G. C., Logan, R. W., & Seney, M. L. (2018). Improved identification of concordant and discordant gene expression signatures using an updated rank-rank hypergeometric overlap approach. Scientific Reports, 8(1), 9588.

(6) Fröhlich, A. S., Gerstner, N., Gagliardi, M., Ködel, M., Yusupov, N., Matosin, N., Czamara, D., Sauer, S., Roeh, S., Murek, V., Chatzinakos, C., Daskalakis, N. P., Knauer-Arloth, J., Ziller, M. J., & Binder, E. B. (2024). Single-nucleus transcriptomic profiling of human orbitofrontal cortex reveals convergent effects of aging and psychiatric disease. Nature Neuroscience, 27(10), 2021–2032.

(7) Green, G. S., Fujita, M., Yang, H.-S., Taga, M., Cain, A., McCabe, C., Comandante-Lou, N., White, C. C., Schmidtner, A. K., Zeng, L., Sigalov, A., Wang, Y., Regev, A., Klein, H.-U., Menon, V., Bennett, D. A., Habib, N., & De Jager, P. L. (2024). Cellular communities reveal trajectories of brain ageing and Alzheimer's disease. Nature, 633(8030), 634–645.

(8) Hannon, E., Dempster, E. L., Davies, J. P., Chioza, B., Blake, G. E. T., Burrage, J., Policicchio, S., Franklin, A., Walker, E. M., Bamford, R. A., Schalkwyk, L. C., & Mill, J. (2024). Quantifying the proportion of different cell types in the human cortex using DNA methylation profiles. BMC Biology, 22(1), 17.

(9) Johnson, E. C. B., Carter, E. K., Dammer, E. B., Duong, D. M., Gerasimov, E. S., Liu, Y., Liu, J., Betarbet, R., Ping, L., Yin, L., Serrano, G. E., Beach, T. G., Peng, J., De Jager, P. L., Haroutunian, V., Zhang, B., Gaiteri, C., Bennett, D. A., Gearing, M., … Seyfried, N. T. (2022). Large-scale deep

multi-layer analysis of Alzheimer's disease brain reveals strong proteomic disease-related changes not observed at the RNA level. Nature Neuroscience, 25(2), 213–225.

(10) Johnson, E. C. B., Dammer, E. B., Duong, D. M., Ping, L., Zhou, M., Yin, L., Higginbotham, L. A., Guajardo, A., White, B., Troncoso, J. C., Thambisetty, M., Montine, T. J., Lee, E. B., Trojanowski, J. Q., Beach, T. G., Reiman, E. M., Haroutunian, V., Wang, M., Schadt, E., … Seyfried, N. T. (2020). Large-scale proteomic analysis of Alzheimer's disease brain and cerebrospinal fluid reveals early changes in energy metabolism associated with microglia and astrocyte activation. Nature Medicine, 26(5), 769–780.

(11) Maitra, M., Mitsuhashi, H., Rahimian, R., Chawla, A., Yang, J., Fiori, L. M., Davoli, M. A., Perlman, K., Aouabed, Z., Mash, D. C., Suderman, M., Mechawar, N., Turecki, G., & Nagy, C. (2023). Cell type specific transcriptomic differences in depression show similar patterns between males and females but implicate distinct cell types and genes. Nature Communications, 14(1), 2912.

(12) Mathys, H., Boix, C. A., Akay, L. A., Xia, Z., Davila-Velderrain, J., Ng, A. P., Jiang, X., Abdelhady, G., Galani, K., Mantero, J., Band, N., James, B. T., Babu, S., Galiana-Melendez, F., Louderback, K., Prokopenko, D., Tanzi, R. E., Bennett, D. A., Tsai, L.-H., & Kellis, M. (2024). Single-cell multiregion dissection of Alzheimer's disease. Nature, 632(8026), 858–868.

(13) Novotny, B. C., Fernandez, M. V., Wang, C., Budde, J. P., Bergmann, K., Eteleeb, A. M., Bradley, J., Webster, C., Ebl, C., Norton, J., Gentsch, J., Dube, U., Wang, F., Morris, J. C., Bateman, R. J., Perrin, R. J., McDade, E., Xiong, C., Chhatwal, J., … Harari, O. (2023). Metabolomic and lipidomic signatures in autosomal dominant and late-onset Alzheimer's disease brains. Alzheimer's & Dementia: The Journal of the Alzheimer's Association, 19(5), 1785–1799.

(14) Plaisier, S. B., Taschereau, R., Wong, J. A., & Graeber, T. G. (2010). Rank-rank hypergeometric overlap: identification of statistically significant overlap between gene-expression signatures. Nucleic Acids Research, 38(17), e169.

(15) Shireby, G., Dempster, E. L., Policicchio, S., Smith, R. G., Pishva, E., Chioza, B., Davies, J. P., Burrage, J., Lunnon, K., Seiler Vellame, D., Love, S., Thomas, A., Brookes, K., Morgan, K., Francis, P., Hannon, E., & Mill, J. (2022). DNA methylation signatures of Alzheimer's disease neuropathology in the cortex are primarily driven by variation in non-neuronal cell-types. Nature Communications, 13(1), 5620.

(16) Tasaki, S., Xu, J., Avey, D. R., Johnson, L., Petyuk, V. A., Dawe, R. J., Bennett, D. A., Wang, Y., & Gaiteri, C. (2022). Inferring protein expression changes from mRNA in Alzheimer's dementia using deep neural networks. Nature Communications, 13(1), 655.

(17) Varma, V. R., Wang, Y., An, Y., Varma, S., Bilgel, M., Doshi, J., Legido-Quigley, C., Delgado, J. C., Oommen, A. M., Roberts, J. A., Wong, D. F., Davatzikos, C., Resnick, S. M., Troncoso, J. C., Pletnikova, O., O'Brien, R., Hak, E., Baak, B. N., Pfeiffer, R., … Thambisetty, M. (2021). Bile acid synthesis, modulation, and dementia: A metabolomic, transcriptomic, and pharmacoepidemiologic study. PLoS Medicine, 18(5), e1003615.

(18) Wan, Y.-W., Al-Ouran, R., Mangleburg, C. G., Perumal, T. M., Lee, T. V., Allison, K., Swarup, V., Funk, C. C., Gaiteri, C., Allen, M., Wang, M., Neuner, S. M., Kaczorowski, C. C., Philip, V. M., Howell, G. R., Martini-Stoica, H., Zheng, H., Mei, H., Zhong, X., … Logsdon, B. A. (2020). Meta-Analysis of the Alzheimer's Disease Human Brain Transcriptome and Functional Dissection in Mouse Models. Cell Reports, 32(2), 107908.

https://doi.org/10.7554/eLife.111228.1.sa0